AD_____

Award Number: DAMD17-99-1-9291

TITLE: A Novel Signaling Perturbation and Ribozyme Gene Therapy Procedure to Block Rho-Kinase (ROK) Activation and Breast Tumor Metastasis

PRINCIPAL INVESTIGATOR: Lilly Y.W. Bourguignon, Ph.D.

CONTRACTING ORGANIZATION: University of Miami Medical School
Miami, Florida 33136

REPORT DATE: September 2001

TYPE OF REPORT: Annual

PREPARED FOR: U.S. Army Medical Research and Materiel Command
Fort Detrick, Maryland 21702-5012

REPORT DOCUMENTATION PAGE

Form Approved
OMB No. 074-0188

1. AGENCY USE ONLY (Leave blank)	2. REPORT DATE	3. REPORT TYPE AND DATES COVERED
	September 2001	Annual (1 Sep 00 - 31 Aug 01)

4. TITLE AND SUBTITLE
A Novel Signaling Perturbation and Ribozyme Gene Therapy Procedure to Block Rho-Kinase (ROK) Activation and Breast Tumor Metastasis

5. FUNDING NUMBERS
DAMD17-99-1-9291

6. AUTHOR(S)
Lilly Y.W. Bourguignon, Ph.D.

7. PERFORMING ORGANIZATION NAME(S) AND ADDRESS(ES)
University of Miami Medical School
Miami, Florida 33136

E-Mail: lillyb@itsa.ucsf.edu

8. PERFORMING ORGANIZATION REPORT NUMBER

9. SPONSORING / MONITORING AGENCY NAME(S) AND ADDRESS(ES)
U.S. Army Medical Research and Materiel Command
Fort Detrick, Maryland 21702-5012

10. SPONSORING / MONITORING AGENCY REPORT NUMBER

11. SUPPLEMENTARY NOTES

12a. DISTRIBUTION / AVAILABILITY STATEMENT
Approved for Public Release; Distribution Unlimited

12b. DISTRIBUTION CODE

13. ABSTRACT *(Maximum 200 Words)*

Breast tumor cells (SP-1) express a major cell adhesion molecule, CD44v10, which binds the extracellular matrix component, hyaluronan (HA), at its external domain and interacts with various signaling molecules at its cytoplasmic domain. In this study we have determined that CD44v10 and Rho-Kinase (ROK) are physically associated as a complex *in vivo*. Using a recombinant fragment of ROK [in particular, the pleckstrin homology (PH) domain] and *in vitro* binding assays, we have detected a specific binding interaction between the PH domain of ROK and the cytoplasmic domain of CD44. Scatchard plot analysis indicates that there is a single high affinity CD44 binding site in the PH domain of ROK with an apparent dissociation constant (Kd) of 1.76nM which is comparable to CD44 binding (Kd ~1.56nM) to intact ROK. These findings suggest that the PH domain is the primary ROK binding region for CD44.

Furthermore, HA binding to SP-1 cells promotes RhoA-mediated ROK activity which, in turn, increases phosphorylation of three different inositol 1, 4, 5-trisphosphate receptors (IP_3Rs) [in particular, subtype 1 (IP_3R1), and to a lesser extent subtype 2 (IP_3R2) and subtype 3 (IP_3R3)] all known as IP_3-gated Ca^{2+} channels. The phosphorylated IP_3R1 (but not IP_3R2 and IP_3R3) is enhanced in its binding to IP_3 which subsequently stimulates IP_3-mediated Ca^{2+} flux. Transfection of SP-1 cells with ROK's PH cDNA significantly reduces ROK association with CD44v10, and effectively inhibits ROK-mediated phosphorylation of IP_3Rs and IP_3R-mediated Ca^{2+} flux *in vitro*. The PH domain of ROK also functions as a dominant-negative mutant *in vivo* to block HA-dependent, CD44v10-specific intracellular Ca^{2+} mobilization and breast tumor cell migration. Taken together, we believe that CD44v10 interaction with ROK plays a pivotal role in IP_3R-mediated Ca^{2+} signaling during HA-mediated breast tumor cell migration.

14. SUBJECT TERMS	15. NUMBER OF PAGES
Breast Cancer	39
	16. PRICE CODE

17. SECURITY CLASSIFICATION OF REPORT	18. SECURITY CLASSIFICATION OF THIS PAGE	19. SECURITY CLASSIFICATION OF ABSTRACT	20. LIMITATION OF ABSTRACT
Unclassified	Unclassified	Unclassified	Unlimited

FOREWORD

Opinions, interpretations, conclusions and recommendations are those of the author and are not necessarily endorsed by the U.S. Army.

___ Where copyrighted material is quoted, permission has been obtained to use such material.

___ Where material from documents designated for limited distribution is quoted, permission has been obtained to use the material.

___ Citations of commercial organizations and trade names in this report do not constitute an official Department of Army endorsement or approval of the products or services of these organizations.

N/A In conducting research using animals, the investigator(s) adhered to the "Guide for the Care and Use of Laboratory Animals," prepared by the Committee on Care and use of Laboratory Animals of the Institute of Laboratory Resources, national Research Council (NIH Publication No. 86-23, Revised 1985).

X For the protection of human subjects, the investigator(s) adhered to policies of applicable Federal Law 45 CFR 46.

X In conducting research utilizing recombinant DNA technology, the investigator(s) adhered to current guidelines promulgated by the National Institutes of Health.

X In the conduct of research utilizing recombinant DNA, the investigator(s) adhered to the NIH Guidelines for Research Involving Recombinant DNA Molecules.

N/A In the conduct of research involving hazardous organisms, the investigator(s) adhered to the CDC-NIH Guide for Biosafety in Microbiological and Biomedical Laboratories.

Lilly Y.W. Bourguignon 11/30/01

PI - Signature Date

Table of Contents

INTRODUCTION

CD44 belongs to a family of transmembrane glycoprotein which is expressed in a variety of cells including breast tumor cells (1-7). To date, multiple CD44 isoforms have been identified (1-7). Some of these isoforms result from extensive, alternative exon splicing events (3-7). Most often, the alternative splicing occurs between exons 5 and 15 leading to an insertion in tandem of one or more variant exons (v1-v10, or exons 6 through exons 14 in human cells) within the membrane proximal region of the extracellular domain (3). The variable primary amino acid sequence of different CD44 isoforms is further modified by extensive N-and O-glycosylations and glycosaminoglycan (GAG) additions (8,9). The extracellular domain of CD44 containing clusters of conserved basic residues (10) plays an important role in the binding of HA, whereas the cytoplasmic domain of CD44 (approximately 70 a. a. long) is both structurally and functionally linked to the cytoskeleton and signaling molecules (11-13).

Our previous studies have shown that cells from different origins all contain a CD44-related transmembrane glycoprotein, named GP116, which contains a v10 exon-coded structure (1). GP116 (also designated as CD44v10) functions as a major hyaluronan (HA) receptor in many different cells (1,2,5). The cytoplasmic domain of CD44v10 serves as one of the cellular substrates for protein kinase C (PKC). In particular, CD44v10 phosphorylation by PKC enhances its interaction with the cytoskeletal protein, ankyrin (11). These observations suggest that CD44 not only functions as an adhesion protein, but may also play an important role as a signal-transducing molecule. The signaling properties of CD44 appear to be required for a variety of cellular activities including cell migration (9,14). Nevertheless, the mechanism by which CD44 mediates cell migration remains to be determined.

Rho-Kinase (also called Rho-Binding Kinase or ROK) is a serine/threonine kinase that is composed of four functional domains: a kinase domain (catalytic site), a coiled-coil domain, a Rho-binding (RB) domain and a pleckstrin-homology (PH) domain (15,16). Both the kinase and Rho-binding (RB) domains share a large amount of sequence homology with a family of related kinases known to bind Rho GTPase and participate in cell motility and cytoskeleton functions (15-18). ROK activity is activated by binding to Rho, and inhibited by certain protein kinase inhibitors (18). The kinase activity appears to be essential for ROK's involvement in promoting stress fiber formation and focal adhesion complexes (16,18). Microinjection of an expression vector encoding ROK results in the formation of stress fibers and focal adhesion complexes in certain cell types (18). In particular, the N-terminal region of ROK is needed for the proper regulation of its activity (18). Truncation of the kinase domain at the N-terminal region results in an inhibition of kinase activity, loss of stress fibers and reduction in focal adhesion complexes (18). The C-terminal sequence [containing both the Rho-binding (RB) domain and the pleckstrin homology (PH) domain] of ROK is also important for the activation of ROK activity in the presence of the GTP-bound form of RhoA (16,18). For example, point mutations of either RB and/or PH domains at the C-terminal region of ROK have been shown to block the formation of stress fiber and focal adhesion (16). These observations suggest that RB and/or PH domain(s) play(s) an important role in regulating ROK activation. Moreover, ROK has been shown to phosphorylate a number of cellular substrates including myosin light chain (17), myosin light chain phosphatase (19), calponin (20), adducin (21) and LIM kinase (22). RhoA-activated ROK also phosphorylates the cytoplasmic domain of CD44v3 isoform and up-regulates the interaction

between CD44v3 isoform and the cytoskeletal protein, ankyrin during breast tumor cell migration (23). Thus, ROK is one of the important signaling molecules participating in HA-mediated CD44 function (23).

A number of laboratories, including our own, have demonstrated that the binding of HA to CD44-expressing cells promotes intracellular Ca^{2+} mobilization which is a pre-requisite for the onset of a variety of biological activities (24-28). Although the cellular and molecular mechanisms involved in HA/CD44-mediated Ca^{2+} signaling are currently not well understood, one of the likely pathways involves the phosphatidylinositol cascade that leads to Ca^{2+} release from intracellular stores (29,30). In response to different stimuli (including HA), phospholipase C is activated to hydrolyze phosphatidyl 4, 5 bisphosphate into diacylglycerol and inositol 1, 4, 5 trisphosphate (IP_3). IP_3, as a second messenger, binds to the IP_3 receptor (IP_3R) and induces the release of Ca^{2+} from intracellular stores (29,30). The IP_3 receptor is assembled into tetrameric complexes with each subunit containing three major domains: an IP_3-binding domain at the N-terminus; a regulatory domain in the middle portion of the protein (transducing the signal of the IP_3 binding to the Ca^{2+} channel); and the Ca^{2+} channel domain at the C-terminus (30-32). There are at least three subtypes of IP_3R [designated as type 1 (IP_3R1), type 2 (IP_3R2) and type 3 (IP_3R3)] that are encoded by different genes (33-37). All three IP_3Rs contain a great amount of structural homology and functional similarities to IP_3-gated Ca^{2+} channels (33-37).

Specifically, in CD44-expressing cells, RhoA and/or ROK have been shown to be important in a variety of cellular functions including Ca^{2+} regulation (38-40). The questions of whether CD44 and ROK play a direct role in regulating breast tumor cell function; and, if so, which cellular protein(s) is(are) most likely involved in CD44-ROK-regulated Ca^{2+} signaling and breast tumor cell migration are addressed in this study.

BODY

MATERIALS AND METHODS

Cell Culture: Mouse breast tumor cells (e.g. SP-1 cell line; provided by Dr. Bruce Elliott, Department of Pathology and Biochemistry, Queen's University, Kingston, Ontario, Canada) were used in this study. They were grown in RMPI 1640 medium supplemented with 10% fetal bovine serum, folic acid (290mg/l), and sodium pyruvate (100mg/l).

Antibodies and Reagents: Monoclonal rat anti-human CD44 antibody (Clone:020; Isotype: IgG_{2b}; obtained from CMB-TECH, Inc., San Francisco, CA.) used in this study recognizes a common determinant of the CD44 class of glycoproteins including CD44v10. For the preparation of polyclonal rabbit anti-CD44v10 or rabbit anti-Rho-Kinase (ROK) antibody, specific synthetic peptides [~15-17 amino acids unique for either CD44v10 or N-terminus ROK] were prepared, respectively by the Peptide Laboratories using an Advanced Chemtech automatic synthesizer (model ACT350). Conjugated CD44v10 or ROK peptides (to polylysine) were injected into rabbits to raise the antibodies. All antibodies (e.g. anti-CD44v10 or anti-ROK sera) were collected from each bleed and stored at 4°C containing 0.1% azide. All antibodies (e.g. rabbit anti-CD44v10 IgG or rabbit anti-ROK IgGs) were prepared using conventional DEAE-cellulose chromatography and were tested to be monospecific (by immunoblot assays). Three

monoclonal mouse anti-IP_3 receptor subtype antibodies were produced by immunizing with specific peptides unique to each IP_3 receptor subtypes [e.g. IP_3R1 (aa2681-2695); IP_3R2 (aa2687-aa2701); and IP_3R3 (aa2657-aa2671)] coupled to poly-lysine as described previously (41). Mouse monoclonal anti-green fluorescent protein (GFP) was purchased from PharMingen. *Clostridium botulinum* C3 toxin was obtained from List Biological Laboratories, Inc. *Escherichia coli*-derived GST-tagged RhoA was a gift from Dr. Martin Schwartz (Scripps Research Institute, La Jolla, CA).

Cloning, Expression and Purification of CD44 Cytoplasmic Domain (CD44cyt) from E. coli: The cytoplasmic domain of human CD44 (CD44cyt) was cloned into pFLAG-AST using the PCR-based cloning strategy. Using human CD44 cDNA as template, one PCR primer pair (left, FLAG-EcoRI; right, FLAG-XbaI) was designed to amplify complete CD44 cytoplasmic domain. The amplified DNA fragments were one-step cloned into a pCR2.1 vector and sequenced. Then, the DNA fragments were cut out by double digestion with EcoRI and XbaI and subcloned into EcoRI/XbaI double-digested pFLAG-AST (Eastman Kodak Co.-IBI, Rochester, NY) to generate FLAG-pCD44cyt construct. The nucleotide sequence of FLAG/CD44cyt junction was confirmed by sequencing. The recombinant plasmids were transformed to BL21-DE3 to produce FLAG-CD44cyt fusion protein. The FLAG-CD44cyt fusion protein was further purified by anti-FLAG M2 affinity gel column (Eastman Kodak Co.-IBI, Rochester, NY). The nucleotide sequence of primers used in this cloning protocol are:

FLAG-EcoRI: 5'-GAGAATTCGAACAGTCGAAGAAGGTGTCTCTTAAGC-3';
FLAG-XbaI: 5'-AGCTCTAGATTACACCCCAATCTTCAT-3'.

Method for preparing GFP (green fluorescent protein)-tagged dominant-negative form [containing PH domain] of Rho-Kinase (ROK): The cDNA fragment encoding the dominant-negative form of ROK (2719-3237bp, containing the PH sequence) was amplified by RT-PCR using PH-specific primers linked with enzyme (Xho I and Hind III) digestion site, 5'-ATAAGCTTTGCAGTGGATCTTGTAGA-3' and 5'-GCCTCGAGATGCTTTCAGTA CCAAATAGA-3'. PCR product digested with Xho I and Hind III was purified with QIAquick PCR purification Kit (Qiagen). The PH cDNA fragments were cloned into pEGFPC1 vector (Clontech) digested with Xho I and Hind III. The inserted PH sequence was confirmed by nucleotide sequencing analyses. This GFP-PH cDNA was then used for a transient expression in SP-1 cells. The GFP-PH (M.W. ~50kDa) expressed in SP-1 cells was analyzed by SDS-PAGE and immunoblot as described below.

Cell Transfection: To establish a transient expression system, SP-1 cells were transfected with various plasmid DNAs (e.g. GFP-tagged PH cDNA or pEGFPC1 vector alone) using electroporation methods according to those procedures described previously (42). Briefly, SP-1 cells were plated at a density of 2×10^6 cells per 100 mm dish and transfected with 25μg/dish plasmid cDNA using Lipofectamine 2000. Transfected cells were grown in the culture medium containing G418 for at least 3 days. Various transfectants were then analyzed for their protein expression (e.g. ROK-related proteins) by immunoblot, ROK activity and cell migration assays as described below.

Measurement of RhoA Activation: Breast tumor cells (SP-1 cells) (~5.0×10^6 cells) were resuspended in a buffer containing 118 mM KCl, 5 mM NaCl, 0.4 mM $CaCl_2$, 1 mM EGTA, 1.2

mM Mg-acetate, 1.2 mM KH_2PO_4, 25 mM Tris-HCl (pH 7.4), 20 mg/ml BSA. Subsequently, an aliquot of the cell suspension was added to the electroporation cuvette and incubated at 4°C for 30 min followed by adding [^{35}S]GTPγS (12.5 μCi). Subsequently, cells were electroporated at 25 microfarads and 2.0 kV/cm followed by incubating with 50μg/ml HA [in the presence or absence of rat anti-CD44 antibody (50μg/ml) or *Clostridium botulinum* C3 toxin (100μg/ml)] or without any HA treatment at 37°C for 30 min. Subsequently, [^{35}S]GTPγS labeled cells were washed in PBS (pH 7.4) and solubilized in 1.0% NP-40 with 1 mM GTP, 25 mM Mg-acetate and protease inhibitors in PBS (pH 7.4). NP-40 solubilized cells were then incubated with mouse anti-RhoA IgG (5μg/ml) plus goat anti-mouse conjugated beads. The amount of [^{35}S]GTPγS•RhoA associated with anti-RhoA-conjugated immuno-beads was measured by a gamma-counter.

Measurement of IP_3 Production: SP-1 cells [untreated or treated with HA (50μg/ml) for 1 min in the presence or absence of rat anti-CD44 antibody (50μg/ml)] were incubated with 0.2 volumes of perchloric acid at 4°C for 20 min. The solutions were then centrifuged at 2000x g for 20 min. The supernatant is removed and neutralized with KOH. The preparations are centrifuged again at 2000x g at 4°C. The supernatant was collected and IP_3 production was measured using the competitive binding system of Biotrak (Amersham).

Immunoblotting and Immunoprecipitation Techniques: Unlabeled SP-1 cells (or surface biotinylated) were solubilized in 50mM HEPES (pH 7.5), 150mM NaCl, 20mM $MgCl_2$, 1.0% Nonidet P-40 (NP-40), 0.2mM Na_3VO_4, 0.2mM phenylmethylsulfonyl fluoride, 10μg/ml leupeptin, and 5μg/ml aprotinin. The sample was then centrifuged at 14,927x g for 15 min and the supernatant was analyzed by SDS-PAGE in a 5% or 7.5% polyacrylamide gel. Separated polypeptides were then transferred onto nitrocellulose filters. After blocking non-specific sites with 2% bovine serum albumin, the nitrocellulose filters were incubated with each of the specific immuno-reagents [e.g. rat anti-CD44 IgG (5μg/ml), rabbit anti-CD44v10 IgG (5μg/ml), rabbit anti-ROK IgG (5μg/ml), monoclonal antibodies against IP_3R1 (5μg/ml), IP_3R2 (5μg/ml) or IP_3R3 (5μg/ml)] followed by incubating with horseradish peroxidase (HRP)-labeled goat anti-rat IgG, or HRP-labeled goat anti-rabbit IgG or HRP-labeled goat anti-mouse IgG or ExtrAvidin peroxidase (to detect surface-biotinylated proteins). The blots were then developed by the ECL™ system (Amersham Co.). For analyzing the recruitment of endogenous ROK into CD44v10 complex, SP-1 cells [either treated with HA (50μg/ml) or without any HA treatment] were solubilized by 1.0% NP-40 and immunoprecipitated with rat anti-CD44 antibody followed by anti-ROK-mediated immunoblot or immunoprecipitated with rabbit anti-ROK antibody followed by anti-CD44-mediated immunoblot, respectively. In some experiments, SP-1 cells (e.g. untransfected or transfected with GFP-tagged ROK's PHcDNA or vector only) [either treated with HA (50μg/ml) or without any HA treatment] were immunoprecipitated with anti-CD44v10 IgG (or anti-GFP IgG) followed by immunobloting with rabbit anti-ROK IgG (or CD44v10 IgG) for 1h at room temperature followed by incubation with horseradish peroxidase-conjugated goat anti-rabbit IgG (or goat anti-mouse IgG) (1:10,000 dilution) at room temperature for 1 h. Some SP-1 cells (e.g. untransfected or transfected with GFP-tagged ROK's PHcDNA or vector only) were also immunobloted with anti-GFP antibody. These blots were then developed using ECL chemiluminescence reagent (Amersham Life Science, England).

In Vitro Binding of CD44cyt to the PH Fragment of ROK or Intact ROK: Aliquots (0.5-1 ng protein) of purified GFP-tagged PH fragment of ROK (isolated from SP-1 cells) or intact

ROK (purified from SP-1 cells)-conjugated Sepharose beads were incubated in 0.5 ml of binding buffer [20 mM Tris-HCl (pH 7.4), 150 mM NaCl, 0.1% bovine serum albumin and 0.05% Triton X-100] containing various concentrations (10-800 ng/ml) of ^{125}I-labeled the cytoplasmic domain of CD44 (CD44cyt) fusion protein (5,000 cpm/ng protein) at 4°C for 4 h. Specifically, equilibrium-binding conditions were determined by performing a time course (1-10h) of ^{125}I-labeled CD44cyt binding to (the PH fragment of ROK or intact ROK) at 4°C. The binding equilibrium was found to be established when the *in vitro* CD44-(PH fragment of ROK or intact ROK) binding assay was conducted at 4°C after 4 h. Following binding, the PH fragment of ROK/intact ROK-conjugated beads were washed extensively in binding buffer and the beads-bound radioactivity was counted. Non-specific binding was determined using a 50-100-fold excess of unlabeled CD44cyt in the presence of the same concentration of ^{125}I-labeled CD44cyt. Non-specific binding which was approximately 20% of the total binding, was always subtracted from the total binding. Our binding data are highly reproducible. The values expressed in the result section represent an average of triplicate determinations of 3-5 experiments with a standard deviation less than ±5%.

Protein Phosphorylation Assay: The kinase reaction was carried out in 50µl of the reaction mixture containing 40 mM Tris-HCl (pH 7.5), 2 mM EDTA, 1 mM DTT, 7 mM $MgCl_2$, 0.1% CHAPS, 0.1 µM calyculin A, 100 µM [γ-^{32}P]ATP (15-600 mCi/mmol), purified enzymes [e.g. 100ng ROK (isolated from SP-1 cells) and 1 µg cellular proteins (e.g. myelin basic protein, and IP_3 receptor subtypes (IP_3R1,IP_3R2 or IP_3R3)] in the presence or absence of GTPγS•GST-RhoA (or GST-RhoA alone). After incubating at 30°C for 2h, the reaction mixtures were boiled in SDS-sample buffer and subjected to SDS-PAGE. The protein bands were revealed by silver stain and the radiolabeled bands were visualized by fluorography or analyzed by liquid scintillation counting.

Measurement of [^{3}H]-IP_3 Binding: First, SP-1 cells (~3.3 x 10^7 cells) were washed in PBS and solubilized in 1 ml of NP-40 buffer for 1 h at 4°C. Sample was centrifuged at 14,927 x g for 15 min to remove insoluble materials. The resulting supernatant was precleared by incubating with mouse IgG agarose beads for 2 h at 4°C. Subsequently, IP_3R1, IP_3R2 and IP_3R3 were immunoprecipitated with specific monoclonal antibodies against various IP_3 receptors [e.g. anti-IP_3R1 antibody (5µg/ml), anti-IP_3R2 antibody (5µg/ml) or anti-IP_3R3 antibody (5µg/ml)] respectively, followed by the addition of anti-mouse IgG agarose beads for 3-4 h at 4°C. Various IP_3 receptor subtype-containing beads were then washed with RIPA [150 mM NaCl, 50 mM Tris-HCl (pH 7.4), 5 mM EDTA, 1% (v/v) Triton X-100, 0.1% (w/v) SDS] and processed for ROK-mediated phosphorylation (as described above).

To determine [^{3}H]-IP_3 binding, IP_3 receptor subtype (e.g. phosphorylated form using ROK activated by GTPγS•GST-RhoA or unphosphorylated form using ROK treated with GST-RhoA alone of IP_3R1, IP_3R2 or IP_3R3-associated beads) were incubated with a solution containing 25 mM sodium phosphate (pH 7.4), 100 mM KCl, 20 mM NaCl, 1 mM EDTA, 1 mg/ml BSA, 0.05% Triton X-100 and 0.01 mCi [^{3}H]-IP_3 (38 Ci/mmol, Amersham Co.) in the presence of various concentration of unlabeled IP_3 in a final volume of 50 ml at 4°C for 2 h with constant agitation as described previously (43,44). The binding reaction was terminated by adding 200 µl of cold phosphate-buffered saline (pH 7.4) and filtrating through GF/B glass fiber filters (Millipore Co., Bedfored, MA). The filter-associated radioactivity was analyzed by liquid

scintillation counting. The results were expressed as "specific binding". Specifically, the concentration of [^{3}H]-IP_3 was held constant and increasing amounts of unlabeled IP_3 (ranging from 10^{-13} M to 10^{-6} M) were added to adjust the total IP_3 concentration. Non-specific binding was defined as the [^{3}H]-IP_3 binding occurring in the presence of 10^{-6} M unlabeled IP_3. The numbers shown in the results were the averages of triplicate determinants in 3 experiments, which varied by less than 5%.

Reconstitution of IP_3R in Phospholipid Vesicles (Liposomes) and Measurement of $^{45}Ca^{2+}$ Flux: Purified IP_3 receptor subtypes (obtained from anti-IP_3R1, IP_3R2 or IP_3R3 immuno-beads) (50μg/ml) were incorporated into phosphatidylcholine/phosphatidylserine vesicles [a ratio of 1:1 IP_3 receptor:phospholipids] in 1% CHAPS followed by dialysis against a buffer containing 20 mM Tris-HCl (pH 7.4), 100 mM NaCl, 100 mM KCl, for 24-48 h with 4 changes of buffer as described previously (43,44). These IP_3 receptor subtype-containing phospholipid vesicles (liposomes) were then processed for phosphorylation (in the presence of ROK activated by GTPγS•GST-RhoA or ROK treated with GST-RhoA alone) and used for the measurement of IP_3-induced Ca^{2+} influx. The Ca^{2+} flux measurement was initiated by adding 2 μCi of $^{45}Ca^{2+}$ (ICN Pharmaceuticals Inc., Costa Mesa, CA) to the IP_3 receptor subtype-containing liposomes in 20 mM Tris-HCl (pH 7.4), 100 mM NaCl, 100 mM KCl, in the presence or absence of IP_3 (1 μM) at 30°C, in a final volume of 50 μl. The Ca^{2+} flux measurement was terminated by adding 3 fold excess of 0.5 mM $CaCl_2$, 5 mM $MgSO_4$ and 100 μg/ml heparin and external $^{45}Ca^{2+}$ was removed by filtration using HAWP filters (0.45 μm, Millipore). After extensive wash with 20 mM Tris-HCl (pH 7.4), 100 mM NaCl, 100 mM KCl, filter-associated radioactivity was determined by liquid scintillation counting.

Measurement of Intracellular Ca^{2+} Mobilization: SP-1 cells (10^7 cells/ml) (e.g. untransfected or transfected with GFP-tagged ROK's PHcDNA or vector only) [pre-treated with various agents such as anti-CD44 antibody (50μg/ml) or Xestospongin C (10μM) or *Clostridium botulinum* C3 toxin (100μg/ml) or without treatment] were first incubated with 10μM Fura-2/AM (Calbiochem) for 1h at room temperature in a buffer solution containing 145 mM NaCl, 5mM KCl, 0.1mM $MgCl_2$, 5mM glucose and 15mM HEPES (pH 7.3) in the presence or absence of 1mM $CaCl_2$. Cells were subsequently washed three times with the same buffer. Cells (10^7 cells/ml) [with or without rat anti-CD44 antibody (50μg/ml)] resuspended in 0.1M phosphate saline buffer (pH 7.0) were incubated simultaneously with an equal volume of 0.1M phosphate saline buffer (pH 7.0) containing hyaluronan (HA) (50μg/ml) (Sigma Chemical Co.) into a 20 microliter chamber alternately illuminated with 200-ms flashes of 340 nm and 380 nm every 10 milliseconds (monitoring the emission wavelength of 510nm) using a Dural-wavelength Fluorescence Imaging System (Intracellular Imaging Inc., Cincinnati, OH). The concentration of intracellular Ca^{2+} was determined by the following equation: $Ca^{2+} = K_d*((R-R_{min})/(R_{max}-R))*F/B$ where Ca^{2+} is intracellular Ca^{2+}, K_d is the dissociation constant of Fura-2 for Ca^{2+}, R is the ratio of the Fura-2 fluorescence excited at 340 divided by the fluorescence excited at 380 nm, R_{min} and R_{max} minimal and maximal fluorescence ratios respectively obtained in ionomycin in the presence of 7 mM EGTA or 2.0 mM Ca^{2+}. F and B are the fluorescence voltage signals at 380 nm in 5.0μM ionomycin in the presence of 7 mM EGTA and 2 mM Ca^{2+}, respectively.

Analyses of *In Vivo* Phosphorylation of IP_3 Receptor Subtypes: To metabolically label cellular phosphoproteins, SP-1 cells (1 x 10^6 cells/ml) (untransfected, vector-transfected or

ROK-PHcDNA-transfected) were washed with phosphate-free DME, and $H_3{}^{32}PO_4$ (carrier free, ICN) was then added at 0.25mCi/ml. After 1h incubation with $H_3{}^{32}PO_4$ at 37°C (isotopic equilibrium inside the cell was reached under this condition), cells were incubated with 50μg/ml HA or without any HA. Subsequently, cells were solubilized by 1% NP-40 and immunoprecipitated with anti-IP_3R1, anti-IP_3R2 or IP_3R3 antibody followed by goat-anti-mouse IgG-conjugated beads. These immunoprecipitated materials were then boiled in SDS-sample buffer and subjected to SDS-PAGE. The protein bands were revealed by silver stain and the radiolabeled bands were visualized by fluorography or analyzed by liquid scintillation counting.

Cell Migration Assay: Twenty-four transwell units were used for monitoring *in vitro* cell migration as described previously (45-47). Specifically, the 8 μm porosity polycarbonate filters were used for the cell migration assay (45-47). SP-1 cells [~1 x 10^4 cells/well in phosphate buffered saline (PBS), pH 7.2] [in the presence or absence of rat anti-CD44 antibody (50μg/ml) or various agents such as Xestospongin C (1μM), BAPTA/AM (1μM), cytochalasin D (20μg/ml), colchicine (1 x 10^{-5}M) or W-7 (1μM)] were placed in the upper chamber of the transwell unit. In some cases, SP-1 cells were transfected with either GFP-tagged PH cDNA or pEGFPC1 vector alone. The medium containing high glucose DMEM supplemented with 50μg/ml hyaluronan was placed in the lower chamber of the transwell unit. After 18 h incubation at 37°C in a humidified 95% air/5% CO_2 atmosphere, vital stain MTT (Sigma Co., St. Louis, MO) was added at a final concentration of 0.2 mg/ml to both the upper and the lower chambers and incubated for additional 4 hours at 37°C. Migratory cells at the lower part of the filter were removed by swabbing with small pieces of Whatman filter paper. Both the polycarbonate filter and the Whatman paper were placed in dimethylsulfoxide to solubilize the crystal. Color intensity was measured in 570 nm. Cell migration was determined by measuring the % of total cells that migrated to the lower side of the polycarbonate filters by standard cell number counting methods as described previously (45-47). The CD44-specific cell migration was determined by subtracting non-specific cell migration (i.e. cells migrate to the lower chamber in the presence of rat anti-CD44 antibody treatment) from the total migratory cells in the lower chamber. Each assay was set up in triplicate and repeated at least 3 times. All data were analyzed statistically using the Student's t test and statistical significance was set at $p<0.01$.

RESULTS

Characterization of CD44v10 Expression in Aortic Endothelial Cells:

The CD44 family of hyaluronan receptor(s) has been found to have an important function in endothelial cell proliferation and migration (48-50). One of the major isoforms of CD44 expressed in breast tumor cells (SP-1 cells) is CD44v10 (also called GP116) (1,2). Using a monoclonal rat anti-CD44 antibody (recognizing a common determinant of the CD44 class of glycoproteins, including various variant isoforms) (Fig. 1, lane 1) and immunoblot analyses, we have confirmed the presence of the 116kDa protein which displays immunological cross-reactivity with CD44 in SP-1 cells. In particular, the anti-CD44v10 antibody is capable of specifically immunoprecipitating the surface-biotinylated 116kDa protein (Fig. 1, lane 2) further confirming that the CD44v10 protein is expressed on the surface of SP-1 cells. No CD44-containing material is observed in control samples when normal rat IgG or preimmune rabbit IgG is used in these experiments (Fig. 1, lane 3 or lane 4). The v10 (or exon 14) inserted structure in

the CD44v10 isoform has been shown to undergo extensive post-translational modification (e.g. N-/O-linked glycosylation and chondroitin sulfate addition, etc.) and participates in HA-dependent biological activities (1,2). The question regarding which signaling pathway(s) is(are) involved in regulating HA/CD44v10-mediated breast tumorl cell function is the focus of this study.

HA-CD44v10-Mediated RhoA Activation in SP-1 Cells:

CD44 signaling is known to be closely associated with changes in certain RhoGTPases such as RhoA (23,50) and Rac1 (47,51,52). RhoA is not only required for actin filament organization and acto-myosin-based contractility (23,53), but can also be physically linked to certain CD44v isoforms in tumor cells (23). Using an *in vitro* [^{35}S]GTPγS binding assay, we have determined that RhoA isolated from SP-1 cells displays guanine nucleotide binding activity (Fig. 2). In particular, the addition of HA to CD44v10-containing SP-1 cells causes an increased level of [^{35}S]GTPγS•RhoA (Fig. 2b) (more than a 3-fold increase) as compared with the amount of [^{35}S]GTPγS•RhoA detected in untreated cells (Fig. 2a), or cells treated with HA in the presence of anti-CD44v10 antibody (Fig. 2d). RhoA is also known to be a substrate for bacterial toxins such as *Clostridium botulinum* C3 toxin (54,55) which ADP-ribosylates RhoA and inactivates RhoA GTPase (54,55). In this study we have found that C3 toxin treatment significantly inhibits the ability of SP-1 cells to form [^{35}S]GTPγS•RhoA during HA treatment (Fig. 2c). These findings suggest that HA and CD44v10 are involved in the activation of RhoA [by stimulating the conversion of inactive RhoA (i.e. little GTP association) into an active form (GTP-bound form)] in breast tumor cells (SP-1).

Detection of A Complex Containing CD44v10 and ROK in SP-1 Cells *in vivo:*

One of the known downstream cellular targets for the GTP-bound (activated) form of RhoA is the serine/threonine kinase, Rho-Kinase (ROK) (15). In this study we have addressed the question of whether there is an interaction between the CD44v10 isoform and ROK in breast tumor cells (SP-1 cells). To this end we first analyzed ROK expression in SP-1 cells. Immunoblot analysis, utilizing anti-ROK antibody designed to recognize the specific epitope located at the N-terminal sequence of ROK, reveals a major protein band (M.W. ~160kDa) (Fig. 3, lane 2). We then demonstrated that the ROK detected in SP-1 cells as revealed by anti-ROK-mediated immunoblot is specific since no protein is detected in these cells using preimmune rabbit IgG (Fig. 3, lane 1). Furthermore, we have carried out anti-CD44v10-mediated and anti-ROK-mediated precipitation followed by anti-ROK immunoblot (Fig. 3, lane 3) or anti-anti-CD44v10 immunoblot (Fig. 3, lane 4), respectively, using SDS-PAGE analyses. Our results clearly indicate that the ROK band is present in the anti-CD44v10-immunoprecipitated materials (Fig. 3, lane 3). The CD44v10 band can also be detected in the anti-ROK-immunoprecipitated materials (Fig. 3, lane 4). These findings clearly establish the fact that CD44v10 and ROK are closely associated with each other *in vivo* in the breast tumor cells.

Interaction Between the PH Domain of ROK and CD44:

The pleckstrin homology (PH) domain is often required membrane localization of a number of signaling molecules (56). To test whether the PH domain of ROK is involved in the

direct binding to CD44, we have used purified green fluorescence protein (GFP)-tagged PH fusion protein of ROK and the FLAG-tagged cytoplasmic domain of CD44 (FLAG-CD44cyt) fusion protein to identify the ROK binding site on the CD44 molecule. Specifically, we have tested the binding of ROK's PH fragment (or the intact ROK) to ^{125}I-labeled FLAG-CD44cyt under equilibrium binding conditions. Scatchard plot analyses presented in Fig. 4 indicate that the cytoplasmic domain of CD44 (CD44cyt) binds to the PH fragment of ROK at a single site (Fig. 4A) with high affinity [an apparent dissociation constant (K_d) of ~1.76nM]. This interaction between CD44 and ROK's PH domain is comparable in affinity to CD44 binding (Kd ~1.56nM) to intact ROK (Fig. 4B). These findings clearly indicate that ROK and, in particular, the PH domain contains the CD44 binding site.

In order to further analyze the interaction between the PH domain of ROK and CD44v10 *in vivo*, we have constructed the PH fragment of ROKcDNA which encodes for the 211 amino acids (aa1143-aa1354) of ROK's PH domain (Fig. 5A-a and 5A-b). This construct was then cloned into a green fluorescent protein (GFP)-tagged expression vector (pEGFPC1 vector) followed by a transient transfection of GFP-tagged PH cDNA (or GFP-tagged vector alone) into SP-1 cells. By carrying out an anti-GFP-immunoblot of SP-1 cells transfected with GFP-tagged PHcDNA (or GFP-vector alone), we have detected the expression of the 50kDa PH domain of ROK (Fig. 5B-a, lane 2) and the 27kDa GFP polypeptide (Fig. 5B-a, lane 1), respectively. When these transfectants were immunoprecipitated by anti-GFP antibody followed by anti-CD44v10 immunoblot, we have determined that CD44v10 is preferentially co-precipitated with the GFP-tagged PH fragment of ROK from cells transfected with GFP-PHcDNA (Fig. 5B-b, lane 2). No detectable CD44v10 is found in anti-GFP-mediated immunoprecipitated materials isolated from pEGFPC1 vector -transfected cells (Fig. 5B-b, lane 1). These results indicate that the PH domain of ROK is also complexed with CD44v10 *in vivo*. Moreover, we have demonstrated that HA is capable of promoting the recruitment of endogenous ROK into a complex with CD44v10 in untransfected (Fig. 5C, lane 1 and 2) or vector-transfected SP-1 cells (Fig. 5C, lane 3 and 4). In contrast, transfection of SP-1 cells with ROK's PHcDNA causes a significant inhibition of HA-mediated recruitment of endogenous ROK to CD44v10 (Fig. 5C, lane 5 and 6). These findings suggest that the ROK fragment containing the PH domain acts as a potent competitive inhibitor for endogenous ROK binding to CD44v10 *in vivo*.

ROK-Mediated Phosphorylation of IP_3 Receptors and Its Role In HA-Mediated Ca^{2+} Signaling:

Activation of CD44 by HA increases intracellular Ca^{2+} mobilization in certain cell types (24). In this study we have used a fluorescence indicator, Fura-2, to measure the intracellular free Ca^{2+} concentration after HA binding to CD44v10-containing SP-1 cells. The ratio of the fluorescence signal from Fura-2 (at 340 and 380 nm excitation) was monitored and used to determine the intracellular Ca^{2+} concentration. Our results show that intracellular Ca^{2+} concentration is elevated after the addition of HA to the breast tumor cells followed by continuous Ca^{2+} influx (Fig. 6A-a). These data indicate that intracellular Ca^{2+} mobilization is one of the early signaling events to occur following HA binding to SP-1 cells. Pretreatment of the cells with anti-CD44v10 effectively blocks HA-mediated Ca^{2+} elevation (Fig. 6A-b) suggesting that Ca^{2+} signaling in these cells undergoes a HA-dependent and CD44v10-specific process.

The production of IP_3 is thought to be required for inducing internal Ca^{2+} release (29) in a variety of cells. Here, we have determined that the stimulation of IP_3 production occurs immediately after HA addition to CD44v10-expressing SP-1 cells (Fig. 6B-a and b). Preincubation with anti-CD44v10 antibody blocks the IP_3 production in SP-1 cells treated with HA (Fig. 6B-c) which indicates that HA induces IP_3 production in a CD44v10-dependent manner in breast tumor cells. Using IP_3 receptor subtype-specific antibodies [e.g. anti-IP_3R1 (Fig. 6C, lane 1), anti-IP_3R2 (Fig. 6C, lane 2) or anti-IP_3R3 (Fig. 6C, lane 3)], we have also identified the presence of the three IP_3R subtypes (all display a similar mass of about 260kDa) in SP-1 cells (Fig. 7C). The question of whether one or more of the IP_3 receptors participate in HA and CD44-specific cellular signaling is subsequently addressed in this study.

Recently, several lines of evidence have indicated that certain RhoGTPases (e.g. Cdc42 and Rac) are involved in the stimulation of IP_3 and Ca^{2+} mobilization pathways during exocytosis of secretory granules (57). In this study we have demonstrated that treatment of SP-1 cells with *Clostridium botulinum* C3 toxin, which ADP-ribosylates and inactivates RhoA, inhibits HA-mediated Ca^{2+} mobilization (Fig. 6A-c). These results are consistent with previous observations showing *Clostridium botulinum* C3 toxin blocks the sustained increase in intracellular $Ca^{2+}$of activated T-lymphocytes (58). Moreover, we have observed that SP-1 cells treated with Xetospongin C (a membrane permeable blocker of IP_3-mediated Ca^{2+} release) (59) causes a significant reduction of HA-mediated Ca^{2+} mobilization (Fig. 6A-d). The addition of ionomycin (5μM) reveals that treatment of cells with either *Clostridium botulinum* C3 toxin (Fig. 6A-c) or Xetospongin C (Fig. 6A-d) does not significantly affect internal Ca^{2+} stores. These observations suggest that RhoA activation and IP_3–mediated Ca^{2+}signaling are closely involved in HA-mediated breast cell activation.

In searching for a possible linkage between RhoA signaling and IP_3-mediated Ca^{2+} regulation, we have found that the ROK isolated from breast tumor cells is capable of phosphorylating the IP3 receptors (in particular, IP_3R1 and to a lesser extent IP_3R2 or IP_3R3) in the presence of activated GTPγS•RhoA (Fig. 7A, lane 4-6). The level of ROK-mediated IP_3 receptor phosphorylation becomes non-detectable if GTPγS•RhoA is not present (Fig. 7A, lane 1-3). In addition, we have analyzed the stoichiometry of IP3 receptor phosphorylation by Rho-Kinase (ROK) using myelin basic protein (MBP) as a positive control. As shown in Fig. 7B, ~0.94 mol of phosphate is incorporated into 1 mol of IP_3R1 by ROK in the presence of activated GTPS•GST-RhoA (Fig. 7B-a). In contrast, phosphorylation of IP_3R2 and IP_3R3 is significantly less than IP_3R1 [at most 0.21mole (Fig. 7B-b) or 0.07 mole (Fig. 7B-c) of phosphate incorporated into per mol of IP_3R2 and IP_3R3, respectively using ROK treated with GTPS•GST-RhoA)]. In addition, we have shown that approximately 1.1 mol of phosphate becomes incorporated per mole of myelin basic protein (MBP) by GTPS•GST-RhoA-activated ROK (Fig. 7B-d) incubated under the same conditions. Since the stoichiometry of IP_3R1 phosphorylation by activated ROK is comparable to that of MBP phosphorylation (by activated ROK), we conclude that IP_3R1 is a functional cellular substrate for the Rho-dependent kinases such as ROK *in vitro.*

In addition, our results indicate that the total amount of ^3H-IP_3 binding to the highly phosphorylated form of IP_3R1 (using GTPγS•RhoA-activated ROK) is significantly higher (Fig. 8A-d,e and f) than that detected in the minimally phosphorylated form of IP_3 receptors (using ROK treated with unactivated RhoA) (Fig. 8A-a,b and c). Most importantly, the highly

phosphorylated IP_3R1 (but not IP_3R1 or IP_3R3) (using ROK in the presence of GTPS•RhoA) induces a relatively higher level of IP_3-induced Ca^{2+} flux activity (Fig. 8B-a, indicated by ■) as compared to the minimally phosphorylated IP3R1 (using ROK in the absence of GTPγS•RhoA) (Fig. 8B-a, indicated by □). In contrast, neither IP_3R2 (Fig. 9B-b, indicated by ■) nor IP_3R3 (Fig. 9C-c, indicated by □) in the presence of either activated or unactivated RhoA displays any significant difference in IP_3-mediated Ca^{2+} flux activities. These results clearly support the notion that phosphorylation of IP3 receptors (in particular, IP_3R1 and to a lesser extent IP_3R2 and IP_3R3) by GTPγS•RhoA-activated ROK enhances IP_3 binding and IP_3-mediated Ca^{2+} signaling *in vitro*.

We have also confirmed that phosphorylation of IP_3 receptors occurs *in vivo*. Fig. 9A shows the results of our SDS-PAGE and autoradiographic analyses of the phosphorylated IP_3 receptor subtypes isolated from SP-1 cells (untransfected or vector-transfected) that were briefly labeled with $H_3{}^{32}PO_4$. All three IP_3 receptors display a relatively low level of phosphorylation (Fig. 9A-a, lane 1-3). Interestingly, phosphorylation of IP_3R1 is significantly enhanced during HA treatment (Fig. 9A-a, lane 4). In contrast, neither IP_3R2 (Fig. 9A-a, lane 5) nor IP_3R3 (Fig. 9A-a, lane 6) displays detectable changes in its phosphorylation pattern during HA treatment of SP-1 cells. It is also noted that transfection of SP-1 cells with ROK's PHcDNA not only greatly reduces the ability of IP_3R1 (Fig. 9A-b, lane 4) (together with IP_3R2 and/or IP_3R3) (Fig. 9A-b, lane 5 and 6) to respond to HA-mediated phosphorylation, but also blocks intracellular Ca^{2+} mobilization (Fig. 9B-1 and 2). The addition of ionomycin to these ROK's PHcDNA-transfected cells does not appear to affect the level of Ca^{2+} in the stores (Fig. 9B-2 insert). In the presence of EGTA, ionomycin-induced Ca^{2+} elevation can be readily inhibited (Fig. 9B-2, insert). Therefore, it is very likely that ROK-mediated phosphorylation of IP_3 receptor (in particular, IP_3R1 and to lesser extent IP_3R2 IP_3R3) is participating in HA- mediated Ca^{2+} signaling in breast tumor cells.

Involvement of Ca^{2+} in Regulating HA-Mediated Breast Tumor Cell Migration:

Abnormal cell migration is considered to be one of the key factors in promoting breast tumor progression (60-62). IP_3 receptor-mediated Ca^{2+} mobilization has been implicated in the regulation of a variety of cellular activities (38-40). In this study we have demonstrated that HA does promote breast tumor cell migration (Table 1A). The fact that treatment of SP-1 cells with rat anti-CD44 antibody (but not normal rat IgG) (Table 1A) or various agents such as Xetospongin C (an IP_3 receptor inhibitor) or a membrane permeable Ca^{2+}chelator (BAPTA) (Table 1B), can effectively block HA and CD44-mediated breast tumor cell migration suggests that IP_3 receptor-mediated Ca^{2+} activity is required for HA/CD44-dependent cell migration. In addition, we have determined that certain drugs, such as cytochalasin D (a microfilament disrupting agent known to prevent actin polymerization) and W-7 (a calmodulin inhibitor known to block myosin light kinase (MLCK) which is required for actomyosin contraction) but not colchicine (a microtubule disrupting agent), can significantly inhibit HA and CD44-specific breast tumor cell migration (Table 1B). These observations support the notion that a Ca^{2+}/calmodulin-dependent actomyosin contractile event is required for HA/CD44-mediated breast tumor cell migration. Finally, we have observed that transfection of breast tumor cells with ROK's PHcDNA effectively inhibits HA-dependent and CD44v10-specific breast tumor cell migration (Table 1C). Taken together, we conclude that the PH fragment of ROK functions as a dominant-negative mutant that effectively inhibits HA/CD44v10-induced ROK activation

and IP_3 receptor phosphorylation required for IP_3 receptor-mediated Ca^{2+}signaling and cytoskeleton-regulated breast tumor cell migration.

KEY RESEARCH ACCOMPLISHMENTS:

•We have observed that the interaction between the metastasis-specific molecule, CD44v10 [the hyaluronan (HA) receptor] and Rho-Kinase (ROK) occurs in metastatic breast tumor cells (SP-1 cell line).
•Scatchard plot analysis indicates that there is a single high affinity CD44 binding site in ROK's PH domain with an apparent dissociation constant (Kd) of 1.76nM which is comparable to CD44 binding (Kd ≈1.56nM) to intact ROK. These findings suggest that the PH domain is the primary ROK binding region for CD44.
•Most importantly, the binding of HA to CD44v10 of SP-1 cells stimulates RhoA activation and ROK-mediated phosphorylation of IP_3 receptors, Ca^{2+} mobilization and cytoskeleton-mediated tumor cell migration.
•Transfection of SP-1 cells with ROK's PHcDNA effectively inhibits ROK association with CD44v10 and efficiently blocks tumor behaviors (e.g. ROK-mediated IP3 receptor phosphorylation, IP_3 receptor-mediated Ca^{2+} mobilization and cytoskeleton-mediated tumor cell migration).
•These observations clearly suggest that the transmembrane interaction between CD44 and ROK (in particular, the PH domain of ROK) promotes IP_3 receptor phosphorylation and subsequent IP_3 receptor-mediated Ca^{2+} signaling that is required for cytoskeleton activation and HA-mediated breast tumor cell migration

REPORTABLE OUTCOMES:

•PUBLICATIONS:

Papers:

1.Bourguignon, Lilly Y.W., H. Zhu, L. Shao, and Y.W. Chen. CD44 Interaction With c-Src Kinase Promotes Cortactin-Mediated Cytoskeleton Function and Hyaluronic acid (HA)-Dependent Ovarian Tumor Cell Migration. J. Biol. Chem. 276:7327-7336 (2001).
2.Franzmann, E.J., D.T. Weed, F.J. Civantos, W.J. Goodwin, and Lilly Y.W. Bourguignon. A Novel CD44v3 Isoform Is Involved in Head and Neck Squamous Cell Carcinomous Progression. Otolaryngol Head Neck Surg 124:426-432 (2001).
3. Bourguignon, Lilly Y.W. CD44-Mediated Oncogenic Signaling and Cytoskeleton Activation During Mammary Tumor Progression. Journal of Mammary Gland Biology and Neoplasia (Invited Review Article) 6:287-297 (2001).
4. Lin, S.Y., A., K. Makino, W. Xia, A. Martin, Y. Wen, K.Yin, Lilly Y.W. Bourguignon and M.C. Hung. Nuclear Localization of EGF Receptor and Its Potential New Role As A Transcription Factor. Nature Cell Biol. 3:802-808 (2001).
5.Chang, W., S. Pratt, T.H. Chen, Lilly Y. W.Bourguignon, and D. Shoback. Amino Acids In the Cytoplasmic Carboxyl-Terminus of the Parathyroid Ca^{2+}-Sensing Receptor Mediate Efficient Cell-Surface Expression and Phospholipase C Activation. J. Biol. Chem. (in press, 2001).
6. Bourguignon, Lilly, Keng-hsueh Lan, Patrick Singleton, Shiaw-Yih Lin, Dihua Yu and Mien-

Chie Hung. EGF Receptor in the Nucleus-Re-Emerging Paradigma? Nature Cell Biol. (Letter) (in press, Jan. 2002).
7. Bourguignon, Lilly Y., Hongbo Zhu, Bo Zhou, Falko Diedrich, Patrick, A Singleton and Mien-Chie Hung. Hyaluronan (HA) Promotes CD44v3-Vav2 Interaction With Grb2-p185^{HER2} and Induces Rac1 & Ras Signaling During Ovarian Tumor Cell Migration and Growth. J. Biol. Chem. (in press, Jan. 2002).
8. Turley, E. A., P. W. Nobel and Lilly Y. W. Bourguignon. Signaling Properties of Hyaluronan Receptors. J. Biol. Chem. (Invited Review Article) (in press, 2002).

•Funding applied for based on work supported by this award:

Funded Active Grants:

NCI Grant (2000-2005)"CD44/Variant-Cytoskeleton In Breast Cancer Progression".

NCI Grant (1999-2003) "CD44-p185^{HER2} Interaction In Ovarian Cancer Progression".

NCI Grant (2001-2003) "CD44 Interaction With Cytokine Receptors in Breast Cancer Bone Metastasis"

CONCLUSIONS:

CD44 [a hyaluronan (HA) receptor] denotes a family of transmembrane glycoproteins resulting from alternative splicing of a single gene (3). This molecule is expressed in a variety of cells and tissues including breast carcinomas (1-7). The binding of HA to CD44 promotes breast tumor cell function including cell adhesion, proliferation and migration (1,2,12,13). Several mechanisms for the regulation of HA-dependent/CD44-specific function in various cell types have been suggested. These include modifications by an additional exon-coded structure (via an alternative splicing process) (3), variable N-/O-linked glycosylation on the CD44's extracellular domain (8); and selective interactions of the CD44 cytoplasmic domain with certain cytoskeletal proteins (e.g. ankyrin and ERM) (11-13,63-65) and various signaling molecules [e.g. the Src family tyrosine kinases (66-69), p185^{HER2} (52,70), protein kinase C (PKC) (1,71), RhoA GTPases (23), and the guanine nucleotide exchange factors Tiam1 (46,47) and Vav2 (52)]. However, the specific cellular and molecular mechanism involved in HA-mediated CD44 signaling in breast tumor cells is the focus of this study.

Molecular biological analyses using RT-PCR, Southern blot, Northern blot, cloning and sequence techniques have shown that breast tumor cells express a CD44 variant isoform which contains an exon with significant homology to human CD44v10 (5). In this study we have used both anti-CD44v10-specific immunoblot and surface biotinylation labeling technique to confirm the expression of CD44v10 (with a molecular mass of ~116kDa) on the surface of SP-1 cells (Fig. 1). The external domain of CD44v10 (also called GP116) has been shown to contain both N-/O-linked oligosaccharide chains and chondroitin sulfate attachment sites required for the binding of extracellular matrix components (ECM) such as hyaluronan (HA) (1,2). The cytoplasmic domain of CD44v10 (GP116) interacts with the cytoskeletal protein, ankyrin (1,2). These findings suggest that CD44v10 plays an important role in providing a direct link between

the ECM (e.g. HA) and the cytoskeleton in breast tumor cells.

Members of the Rho subclass of the Ras superfamily [small molecular weight GTPases, (e.g. RhoA, Rac1 and Cdc42)] are known to transduce signals regulating many cellular processes including Ca^{2+} mobilization (57,58) and cell migration (9,14,23). HA-mediated CD44 signaling has been shown to be closely associated with the activation of RhoGTPases (e.g. RhoA and Rac1) in tumor cells (23,46,47,52). In fact, our results confirm that HA treatment of SP-1 cells causes a significant stimulation of RhoA activation (at least three-fold increase) as compared to untreated cells (Fig. 2). Several enzymes have been identified as possible downstream targets for RhoA signaling. One such enzyme is Rho-Kinase (ROK-also called Rho-associated kinase) which is a serine-threonine kinase known to interact with Rho in a GTP-dependent manner (15,16). ROK is composed of four functional domains including a kinase domain (catalytic site), a coiled-coil domain, a Rho-binding (RB) domain and a pleckstrin-homology (PH) domain (17,18). This enzyme has been shown to regulate cytoskeleton function by phosphorylating several important cytoskeletal regulators including myosin light chain (17), the myosin-binding subunit (MBS) of myosin phosphatase (19),calponin (20), adducin (21) and LIM kinase (22). ROK is also involved in the "cross-talk" between Ras and Rho signaling leading to cellular transformation (72). Using a ROK-specific antibody, we have confirmed the presence of ROK in breast tumor cells (SP-1 cells) (Fig. 3). In a previous study we have demonstrated that ROK phosphorylates the cytoplasmic domain of $CD44v_{3,8\text{-}10}$ isoform and up-regulates the interaction between $CD44v_{3,8\text{-}10}$ isoform and the cytoskeletal protein, ankyrin, during HA/CD44-regulated breast tumor cell migration (23). Thus, ROK is considered to be one of the important signaling molecules required for membrane-cytoskeleton interaction and HA/CD44-mediated functions (23).

In general, the pleckstrin homology (PH) domains are known to be involved in protein and lipid interactions and/or the recruitment of signaling molecules to the plasma membrane (56). The PH domain of ROK has been shown to be involved in the regulation of ROK function (18). In Fig. 3 we have detected that ROK is closely associated with CD44v10 as a complex in breast tumor cells (SP-1). Using two recombinant proteins [GFP-tagged PH domain of ROK and FLAG-tagged CD44 cytoplasmic domain (FLAG-CD44cyt)], we have illustrated that the PH domain of ROK is directly involved in the binding to the cytoplasmic domain of CD44 *in vitro* (Fig. 4). The binding affinity of ROK's PH domain to CD44 is comparable to the intact ROK binding to CD44 (Fig. 4). Transfection of SP-1 cells with ROK's PH domaincDNA (Fig. 5A and B), which effectively competes for endogenous ROK binding to the plasma membrane proteins such as CD44v10 (Fig.5D), strongly suggests that ROK's PH is responsible for the recognition of CD44 both *in vivo* and *in vitro*. These results are consistent with our previous study showing a sequence adjacent to the N-terminal region of PH domain (the PHn-CC-EX domain) of Tiam1 [a Rac1-specific guanine nucleotide exchange factor (GEF)] that is involved in the direct binding to CD44v3 isoform during HA stimulated Rac1 signaling and cytoskeleton-mediated tumor cell migration (47). It is therefore, apparent that select interactions between CD44 isoforms and certain PH domain-containing molecules (e.g. Tiam1 and ROK) play an important role in HA signaling.

Intracellular Ca^{2+} is known to play an important role in cell activation and associated functional responses (73-76). In many cells, Ca^{2+} mobilization by physiological stimuli often

appears to be closely associated with the receptor-activated hydrolysis of PIP_2 to diacylglycerol and IP_3 (29-30). Here, we have demonstrated that HA binding to CD44v10-containing SP-1 cells stimulates IP_3 production (Fig.6B) and the onset of intracellular Ca^{2+} mobilization (Fig. 6A). Receptor-stimulated Ca^{2+} mobilization has been suggested to involve an initial release of Ca^{2+} from intracellular stores followed by Ca^{2+} entry from the extracellular space (77,78). The release of Ca^{2+} from internal stores appears to be caused by the specific binding of inositol-1,4,5-triphosphate (IP_3) to its receptor (IP_3-gated Ca^{2+}channels) (29,30).

Biochemical studies have demonstrated the presence of several IP_3 receptors with different IP_3-binding kinetics in a variety of vertebrate cells (33-37). Both molecular cloning data and immunological analyses indicate that there are at least three IP_3 receptor subtypes derived from three distinct genes, designated type 1 (IP_3R1), type 2 (IP_3R2) and type 3 (IP_3R3) (33-37). The three IP_3R subtypes appear to be differentially expressed and regulated in various cell types and mammalian tissues (33-37). Apparently, selective expression and/or regulation of the IP_3 receptor subtypes confer cell-specific regulation on IP_3-induced Ca^{2+} signaling. In breast tumor cells, we have detected the expression of three IP_3 receptor subtypes (Fig. 6C). The IP_3 binding affinity of the three IP_3R subtypes (Fig. 8A) and the ability of these IP_3R subtypes to respond to Ca^{2+}flux by IP_3 (Fig. 8B) is comparable to those reported by other investigators (33-35,44). The fact that a potent IP3 receptor blocker, Xetospongin C, can effectively inhibit HA-induced Ca^{2+} mobilization *in vivo* (Fig. 6A-d) strongly suggests that IP_3 receptors are involved in HA-mediated Ca^{2+} signaling in breast tumor cells.

One important mechanism for regulating IP_3 receptor function is through phosphorylation. It has been found that serine phosphorylation of the IP_3 receptor by protein kinase A (activated by cAMP), protein kinase C (activated by DAG) or Ca^{2+}/calmodulin-dependent protein kinase results in the regulation of IP_3 receptor activity (79-82). In this study we have presented new evidence that ROK is capable of promoting phosphorylation of IP_3 receptors (in particular, IP_3R1 and to a lesser extent IP_3R2 and IP_3R3) (Fig. 7A). Since the stoichiometry of IP_3R1 phosphorylation (~0.94mol of phosphate is maximally incorporated into 1 mol of IP_3R1 by ROK in the presence of activated GTPS•GST-RhoA) (Fig. 7B) is significantly higher than both IP_3R2 and IP_3R3 phosphorylation (at most 0.21mol or 0.07 mol of phosphate incorporated per mol of IP_3R2 and IP_3R3 by activated ROK, respectively), IP_3R1 is clearly the preferred substrate for ROK. Most importantly, ROK-mediated phosphorylation of IP_3R1 up-regulates IP_3-mediated binding (Fig. 8A) and Ca^{2+} flux activity (Fig. 8B). Thus, it appears that ROK-mediated phosphorylation of IP_3 receptor(s) and IP_3 receptor-mediated Ca^{2+} signaling are closely coupled in HA-CD44 interaction.

These results are consistent with previous findings suggesting that Rho and ROK are important for Ca^{2+}sensatization in hamster muscle resistance arteries (83). Using dominant-negative and dominant-active forms of Cdc42 and Rac, Hong-Geller and Cerione have suggested that these small GTPases may regulate signal transduction at the level of PLCγ1 and IP_3 production (57). In this regard, we have observed that transfection of SP-1 cells with a dominant-negative form of ROK (e.g. ROK's PH domain) does not directly affect IP_3 production (preliminary observation). However, overexpression of the PH domain of ROK can effectively block several important cellular events including CD44v10-endogeneous ROK complex formation (Fig. 5D), HA-induced IP_3 receptor phosphorylation (Fig. 9A), intracellular Ca^{2+}

mobilization (Fig. 9B) and breast tumor cell migration (Table 1B).

One of the mechanisms by which Ca^{2+} may trigger early signal transducing events during HA and CD44-mediated cell migration involves its interaction with calmodulin, an ubiquitous Ca^{2+} binding protein (24,84). Ca^{2+} -dependent calmodulin activity is known to be responsible for the activation of a number of important cellular enzymes, including myosin light chain kinase (MLCK) (85-87). Ca^{2+}/calmodulin-dependent phosphorylation of myosin light chain has been shown to be important for breast tumor cell migration (88). The fact that various inhibitors, such as IP_3 receptor blockers, Ca^{2+} chelators, calmodulin inhibitors, and actin-based cytoskeleton inhibitors (but not microtubule-disrupting drugs) can prevent HA and CD44-mediated breast tumor cell migration (Table 1) suggests that the actomyosin contractile system regulated by Ca^{2+} and calmodulin (also possibly myosin light chain kinase) plays an important role in HA-mediated CD44 signaling. Taken together, we would like to propose that the transmembrane interaction between CD44 and ROK (in particular, the PH domain of ROK) promotes IP_3 receptor phosphorylation and subsequent IP_3 receptor-mediated Ca^{2+} signaling that is required for cytoskeleton activation and HA-mediated breast tumor cell migration (Fig. 10).

REFERENCES:

1. Iida, N. and Bourguignon, L.Y.W. (1997) J. *Cell Physiol.* **171,**152-160
2. Bourguignon, L.Y.W., Iida, N., Welsh, C.F., Krongrad, A., Zhu, D. and Pasquale, D. (1995) *J. Neuro-Oncology* **26,**201-208
3. Screaton, G.R., Bell, M.V., Jackson, D.G., Cornelis, F.B., Gerth, U., and Bell, J.I. (1992) *Proc. Natl. Acad. Sci. U.S.A.* **89**, 12160-12164
4. Dall, P., Heider, K.-H., Sinn, H.-P., Skroch-Angel, P., Adolf, G., Kaufmann, M., Herrlich, P. and Ponta, H. (1995) *Int J Cancer* **60,**471-477
5. Iida, N. and Bourguignon, L.Y.W. (1995) *J Cell Physiol* **162:**127-133.
6. Kaufmann, M., Heider, K.H., Sinn, H.P., von Minckwitz, G., Ponta, H., and Herrlich, P. (1995) *Lancet* **345,**615-619
7. Kalish, E., Iida, N., Moffat, F.L., and Bourguignon, L.Y.W. (1999) *Front Biosci* **4:**1-8
8. Lokeshwar, V.B., and Bourguignon, L.Y.W. (1991) *J. Biol. Chem.* **266,**17983-17989
9. Henke, C.A., Roongta, U., Mickelson, Knutson, J.R. and McCarthy, J.B. (1996) *J. Clin. Invest.* **97,**2541-2552.
10. Yang, B., Yang, B.L., Savani, R.C., and Turley, E.A. (1994) *EMBO J.* **13,**286-296
11. Bourguignon, L.Y.W. (1996) *Current Topics in Membranes* (Ed: W.J. Nelson) **43,**293-312
12. Bourguignon, L.Y.W., Zhu, D., and Zhu, H. (1998) *Front Biosci.* **3,**637-649
13. Bourguignon, L.Y.W. (2001) *J. Mammary Gland Biol & Neoplasia* **6,**287-297
14. Trochon, V., Mabilat, C., Bertrand, P., Legrand, Y., Smadja-Joffe, F., Soria, C., Delpech, B., and Lu, H. (1996) *Int. J. Cancer* **66,**664-668
15. Matsui, T., Amano, M., Yamamoto, T., Chihara, K., Nakafuku, M., Ito, M., Nakano, T., Okawa, K., Iwamatsu, A. and Kaibuchi, K. (1996) *EMBO J.* **15,**2208-2216
16. Amano, M., Chihara, K., Nakamura, N., Kaneko, T., Matsuura, Y., and Kaibuchi, K. (1999) *J. Biol. Chem.* **274,**32418-32424
17. Amano, M., Ito, M., Kimura, K., Fukata, Y., Chihara, K., Nakano, T., Matsuura, Y., and Kaibuchi, K. (1996) *J. Biol. Chem.* **271,**20246-20249
18. Amano, M., Chihara, K., Kimura, K. Fukata, Y., Nakamura, N., Matsuura, Y. and Kaibuchi,

K. (1997) *Science* **275,**1308-1311
19. Kimura, N., Ito, M., Amano, M., Chihara, K., Fukata, Y., Nakafuku, M., Yamamori, B., Feng, J., Nakano, T., Okawa, K., Iwamatsu, K. and Kaibuchi, K. (1996) *Science* **273,**245-248
20. Kaneko, T., Amano, M., Maeda, A., Goto, H., Takahashi, K., Ito, M. and Kaibuchi, K. (2000) *Biochem. Biophys. Res. Commun.* **273,**110-116
21. Fukata, Y., Oshiro, N., Kinoshita, N., Kawano, Y., Matsuoka, Y., Bennett, V., Matsuura, Y. and Kaibuchi, K. (1999) *J. Cell Biol.* **145,**347-361
22. Amano, T., Tanabe, K., Eto, T., Narumiya, S. and Mizuno, K. (2001) *Biochem. J.* **354,**149-159
23. Bourguignon, L.Y.W., Zhu, H., Shao, L., Zhu, D. and Chen, Y.W. (1999) *Cell Motil Cytoskel* **43,**269-287
24. Bourguignon, L.Y.W., Lokeshwar, V.B., Chen, X. and Kerrick, W.G.L. (1993) *J. Immunol.* **151,**6634-6644
25. Bourguignon, L.Y.W., Iida, N., Sobrin, L., and Bourguignon, G.J. (1994) *J. Cell Physiol.*, **159,**29-34
26. Galluzo, E., Albi, N., Fiorucci, S., Merigiola, C., Ruggeri, L., Tosti, A., Grossi, C.E., and Velardi, A. (1995) *Eur. J. Immunol.* **25,**2932-2939
27. Bruno, S., Fabbi, M., Tiso, M., Santamaria, B., Ghiotto, F., Saverino, D., Tenca, C., Zarcone, D., Ferrini, E.C., and Grossi, C.E. (2000) *Carcinogenesis* **21,**893-900
28. Partida-Sanchez, S., Garibay-Escobar, A., Frixione, E., Parkhouse, R.M., and Santos-Argumedo, L. (2000) *Eur. J. Immunol.* **30,**2722-2728
29. Berridge, M.J. (1993) *Nature* **361,** 315-325
30. Yoshida, Y., and Imai S. (1997) *Jpn. J. Pharmacol.* **74,**125-137
31. Joseph, S.K. (1996) *Cell. Signal.* **8,**1-7
32. Taylor, C.W., Genazzani, A.A, and Morris, S.A. (1999) *Cell Calcium* **26,**237-251
33. Furuichi T, Yoshikawa S, Miyawaki A, Wada K, Maeda N , Mikoshiba K. (1989) *Nature* **342,**32-38
34. Mignery, G.A., Newton, C.L., Archer III, B.T., Sudhof, T.C.(1990) *J. Biol. Chem.* **265,** 12679-12685
35. Blondel, O., Takeda, J., Janssen, H., Seino, S., Bell, G.I. (1993) *J. Biol. Chem.* **268,**11356-11363
36. Maranto, A.R. (1994) *J. Biol. Chem.* **269,**1222-123
37. Yamamoto-Hino, M., Sugiyama, T., Hikichi, K., Mattei, M. G., Hasegawa, K., Sekine, S., Sakurada, K., Miyawaki, A., Furuichi, T., Hasegawa, M. (1994) *Receptors and Channels* **2,**9-22-
38. Garcia, J.G.N., Verin, A.D., Schaphorst, K., Siddigui, R., Patterson, C.E., Csortos, C., and Natarajan, V. (1999) *Am. J. Physiol.* **276,**L989-L998
39. Masiero, L., Lapidos, K.A., Ambudkar, I., and Kohn, E.C. (1999). *J. Cell Sci.* **112,**3205-3213
40. Martinez, M.C., Randriamboavojy, V., Ohlmann, P., Komas, N., Duark, J., Schneider, F., Stoclet, J. and Andriantsitohaina, R. (2000), *AJP-Heart and Circulatory Physiol.* **279,**H1228-H1238
41. Sugiyama T, Furuya A, Monkawa T., Yamamoto-Hino, M., Satoh, S., Ohmori, K., Miyawaki, A., Hanai, N., Mikoshiba, K., and Hasegawa, M. (1994) *FEBS Lett.* **354,**149-154
42. Chu, G., Hayakawa, H., and Berg, P. (1987*) Nucleic Acid Res.* **15,**1311-1326
43. Ferris, C.D., Huganir, R.L., Supattapone, S., Snyder, S.H. (1989) *Nature* **342,** 87-89
44. Diaz, F. and Bourguignon, L.Y.W. (2000) *Cell Calcium* **27,**315-328
45. Merzak, A., Koochekpour, S., Pilkington, G.J., (1994) *Cancer Res* **54,**3988-3992

46. Bourguignon, L.Y.W., Zhu, H., Shao, L., and Chen, Y.W. (2000) *J. Cell Biol.* **150,**177-191
47. Bourguignon, L.Y.W., Zhu, H., Shao, L., and Chen, Y.W. (2000) *J. Biol. Chem.* **275,**1829-1838.
48. Slevin, M., Krupinski, J., Kumar, S., and Gaffney, J. (1998) *Lab Invest.* **78,**987-1003
49. Griffioen, A.W., Coener, M.J., Damen, C.A., Hellwig, S.M., van Weering, D.H., Vooys, W., Blijham, G.H. and Groeneweger, G. (1997) *Blood*, **90,**150-115
50. Hirao, M., Sato, N., Kondo, T., Yonemura, S., Monden, M., Sasaki, T., Takai, Y.,Tsukita, S., and Tsukita, S. (1966) *J. Cell Biol.* **135,**36-51
51.Oliferenko, S., Kaverina, I., Small, J.V. and Huber, L.A. (2000). *J Cell Biol* **148,**1159-1164
52.Bourguignon, L.Y.W., Hongbo, Z., B. Zhou, F. Diedrich, P.A. Singleton and Hung, M.C. (2002) *J. Biol. Chem* (in press).
53. Hall, A. (1998) *Science* **279,**509-514
54. Aktories, K., Weller, U., Chhatwal, G.S. (1987) *FEBS Letters* **212,**109-113
55. Ohashi, Y. and Narumiya, S. (1987) *J. Biol. Chem.* **262,**1430-1433
56. Lemmon, M.A., Ferguson, K.M., and Schlessinger, J. (1996) *Cell* **85,**621-624
57. Hong-Geller, E. and Ceroine, R.A. (2000*) J. Cell Biol.* **148,**481-493
58. Angkachatchai, V. and Finkel, T.H. (1999*) J. Immunol.* **163,**3819-3825
59. Gafni, J., Munsch, J.A., Lam, T.H., Catlin, M.C., Costa, L.G., Molinski, T.F. and Pessah, I.N. (1997) *Neuron* **19,**723-733
60. Boyle, E.M., Lille, S.T., Allaire, E., Clowes, A.W., and Verrier, E.D. (1997) *Ann.Thoracic Surgery* **63,**885-894
61. Mombouli, J.V. and Vanhoutte, P.M. (1999*) J. Mol. Cell. Cardiol.* **31,**61-74
62. Shimokawa, H. (1999) *J. Mol. Cell. Cardiol.* **31,**23-37
63. Lokeshwar, V.B., Fregien, N. and Bourguignon, L.Y.W. (1994). *J Cell Biol* **126,**1099-1109
64. Zhu, D. and Bourguignon, L.Y.W. (2000). *J Cell Physiol* **183,**182-195
65. Bretscher, A. (1999) *Curr. Opin. Cell Biol.* **11,**109-116
66. Zhu, D. and Bourguignon, L.Y.W. (1998) *Cell Motil Cytoskel* **39,**209-222
67. Bourguignon, L.Y.W., Zhu, H., Shao, L. and Chen, Y.W. (2001) *J Biol Chem* **276,**7327-7336.
68. Taher, T.E., Smit, L., Griffioen, A.W., Schilder-Tol, E.J., Borst, J., Pals, S.T. (1996) *J. Biol.Chem.* **271,**2863-2867
69. Ilangumaran, S., Briol, A. and Hoessli, D.C. (1998) *Blood* **92,**3901-3908
70. Bourguignon, L.Y.W., Zhu, H.B., Chu, A., Zhang, L., and Hung, M.C. (1997) *J Biol Chem* **272,**27913-27918
71. Kalomiris, E.L. and Bourguignon, L.Y.W. (1989). *J. Biol. Chem.* **264,**8113-8119
72. Sahai, E., Olson, M. F. and Marshall, C.J. (2001) *EMBO J.* **20,**755-766
73. Berridge, M.J., Bootman, M.D, Lipp, P. (1998) *Nature* **395,** 645-648
74. Berridge, M.J. (1995) *Cell* **83,**675-678
75. McConkey, D.J. and Orrenius S. (1997) *Biochem. Biophys. Res. Comm.* **239,**357-366
76. Trump, B.F. and Berezesky, I.K. (1996) *Biochim. Biophys. Acta* **1313,**173-178
77. Kiselyov, K.I., Xu, X., Mozhayeva, G.N., Kuo, T., Pessah, I., Mignery, G.A., Zhu, X., Bimbaumer, L., and Muallem, S. (1998) *Nature* **396,**478-482
78. Kiselyov, K., Mignery, G., Zhu, M. X., and Muallem, S. (1999) *Mol. Cell* **4,**423-429
79. Ferris, C.D., Huganis, R.L., Bredt, D.S., Cameron, A.M., and Snyder, S.H. (1991) *Proc Nat Acad Sci (USA)* **88,**2232-2235
80. Matter, N., Ritz, M.F., Freyermuth, S., Rogue, P., and Malviya, A.N. (1993) *J. Biol. Chem.*

268,732-736
81. Zhang, B.X., Zhao, H., and Muallem, S. (1993) *J. Biol. Chem.* **268**,10997-11001
82. Wojcikiewicz, R.J.H. and Luo, S.G. (1998), *J. Biol. Chem.* **273**,5670-5677,
83. Boltz, S.S., Galle, J., Derwand, R., de Wit C., and Pohl, U. (2000) *Circulation* **102**,2402-2410
84. Chin, D. and Means, A.R. (2000) Trends Cell Biol. 10,322-328.
85. Tran, Q.K., Ohashi, K., and Watanabe, H. (2000) *Cardiovas Res* **48**,13-22
86. Kamm, K.E., and Stull, J.T. (2001) *J.Biolo. Chem.* **276**,4527-4530
87. Stull, J.T. (2001) *J.Biol. Chem.* **276**,2311-2312
88. Bourguignon, L.Y.W., Gunja-Smith, Z., Iida, N., Zhu, H.B., Young, L.J.T., Muller, W. and Cardiff, R.D. (1998) *J. Cell. Physiol.* **176**,206-215

APPENDICES:

FIGURE LEGENDS

Fig.1: Characterization of CD44v10 Expression in SP-1 Cells.

Breast tumor cells (SP-1 cells) were surface biotinylated, NP-40 solubilized and immunoblotted/immunoprecipitated by two different anti-CD44 antibodies as described in the Materials and Methods.

Lane 1: Immunoblot of SP-1 cells using monoclonal rat anti-CD44 antibody (recognizing a common determinant of the CD44 class of glycoproteins, including variant isoforms).

Lane 2: Immunoprecipitation of surface biotinylated SP-1 cells using rabbit anti-CD44v10 antibody (recognizing a v10-specific sequence located at the membrane proximal region of CD44's extracellular domain).

Lane 3: Immunoblot of SP-1 cells with normal rat IgG.

Lane 4: Immunoprecipitation of surface biotinylated SP-1 cells with preimmune rabbit IgG.

Fig. 2: Detection of RhoA Activation in SP-1 cells.

SP-1 cells (~5.0 x 10^6 cells) were preloaded with [^{35}S]GTPγS (12.5 μCi) using electroporation methods as described in the Materials and Methods. Subsequently, these cells were incubated with 50μg/ml HA [in the presence or absence of rat anti-CD44 antibody (50μg/ml) or *Clostridium botulinum* C3 toxin (100μg/ml)] or without any HA treatment at 37°C for 30 min. Subsequently, [^{35}S]GTPγS labeled cells were solubilized in 1.0% NP-40 and incubated with mouse anti-RhoA IgG (5μg/ml) plus goat anti-mouse conjugated beads. The amount of [^{35}S]GTPγS•RhoA associated with anti-RhoA-conjugated immuno-beads was measured using a gamma counter.

a: The amount of [^{35}S]GTPγS•RhoA formation in cells without any treatment.

b:The amount of [^{35}S]GTPγS •RhoA formation in cells treated with HA.

c: The amount of [^{35}S]GTPγS •RhoA formation in cells pretreated with *Clostridium botulinum* C3 toxin followed by HA treatment.

d: The amount of [^{35}S]GTPγS•RhoA formation in cells pretreated with anti-CD44v10 antibody followed by HA treatment.

Fig. 3: Detection of ROK and ROK-CD44v10 complex in SP-1 cells.

SP-1 cells were solubilized by 1% Nonidet P-40 (NP-40) buffer followed by Immunoprecipitation and/or immunblot by anti-ROK antibody or anti-CD44v10 antibody, respectively as described in the Materials and Methods.

Lane 1: Immunoblot of SP-1 cells with preimmune rabbit IgG.

Lane 2: Detection of ROK with anti-ROK-mediated immunoblot of SP-1 cells.

Lane 3: Detection of ROK in the complex by anti-CD44v10-immunoprecipitation followed by immunoblotting with anti-ROK antibody.

Lane 4: Detection of CD44v10 in the complex by anti-ROK Immunoprecipitation followed by immunoblotting with anti-CD44v10 antibody.

Fig.4: Binding of ^{125}I-labeled FLAG-CD44cyt to the PH fragment of ROK (or intact ROK).

Various concentrations of ^{125}I-labeled FLAG-CD44cyt were incubated with the PH fragment of ROK (A) or intact ROK (B)-coupled beads at 4°C for 4 h. Following binding, beads were washed extensively in binding buffer and the bead-bound radioactivity was counted. As a control, ^{125}I-labeled FLAG-CD44cyt was also incubated with uncoated beads to determine the binding observed due to the non-specific binding of the ligand. Non-specific binding, which represented approximately 20% of the total binding, was always subtracted from the total binding. The values expressed in the result section represent an average of triplicate determinations of 3-5 experiments with a standard deviation less than ±5%.

Fig. 5: Transfection of SP-1 cells with ROK's PH cDNA.

A: Schematic illustration of both full-length ROK (a) and ROK-PH fragment (b).

B: (a) Detecting the expression of GFP-tagged ROK-PH fragment (lane 2) or GFP alone (lane 1) by anti-GFP-mediated immunoblot, respectively, in the cell lysate obtained from GFP-tagged ROK-PHcDNA (lane 2) or pEGFPC1 vector alone (lane 1).

(b) Detection of CD44v10-GFP-tagged ROK-PH complex formation in SP-1 cells transfected with GFP-tagged ROK-PHcDNA (lane 2) or pEGFPC1 vector alone (lane 1), and analyzed by anti-GFP-mediated Immunoprecipitation and anti-CD44v10-mediated immunoblot.

C: Analysis of the recruitment of ROK into CD44v10 complex.

SP-1 cells [untransfected or transfected with GFP-tagged ROK-PHcDNA or pEGFPC1 vector alone] were either treated with HA or without any HA treatment. These cells were then solubilized by NP-40, and immunopreciptated with anti-CD44v10 antibody followed by immunoblotting with anti-ROK antibody.

Lane 1: Detection of ROK-CD44v10 complex in untransfected cells treated with no HA.

Lane 2: Detection of ROK-CD44v10 complex in untransfected cells treated with HA.

Lane 3: Detection of ROK-CD44v10 complex in pEGFPC1 vector-transfected cells treated with no HA.

Lane 4: Detection of ROK-CD44v10 complex in pEGFPC1 vector-transfected cells treated with HA.

Lane 5: Detection of ROK-CD44v10 complex in GFP-tagged ROK-PHcDNA transfected cells treated with no HA.

Lane 6: Detection of ROK-CD44v10 complex in GFP-tagged ROK-PHcDNA transfected cells treated with HA.

Fig. 6: Measurement of Ca^{2+} mobilization (A), IP_3 Production (B) and IP_3 Receptor Expression in SP-1 cells.

A: Intracellular Ca^{2+} mobilization was measured by a fluorescence spectrophotometer using cells loaded with 10μM Fura-2/AM as described in the Materials and Methods. Subsequently, Fura-2 labeled cells (preincubated with 0.1mM EGTA) were treated with HA (indicated by arrow head) (a); or pretreated with anti-CD44v10 antibody followed by HA treatment (indicated by arrow head) (b); or pretreated with *Clostridium botulinum* C3 toxin (in the presence of low Ca^{2+}) followed by HA treatment (indicated by arrow head) and ionomycin (indicated by arrow) (c) or pretreated with Xetospongin C (in the presence of low Ca^{2+}) followed by HA treatment (indicated by arrow head) and ionomycin (indicated by arrow) (d).

B: SP-1 cells [(untreated or treated with HA (50μg/ml) in the presence or absence of rat anti-CD44 antibody (50μg/ml)] were used to detect IP_3 production using the competitive binding system of Biotrak (Amersham) as described in the Materials and Methods.

a: Cells had no HA treatment.

b: Cells were treated with HA.

c: Cells were pretreated with anti-CD44v10 followed by HA treatment.

C: Characterization of IP_3 Receptor Subtype Expression in SP-1 Cells.

SP-1 cells were solubilized by NP-40 and immunobloted with IP_3 receptor subtype-specific antibodies as described in the Materials and Methods.

Lane 1: Immunoblot of SP-1 cells using monoclonal mouse anti-IP_3R1 antibody.

Lane 2: Immunoblot of SP-1 cells using monoclonal mouse anti-IP_3R2 antibody.

Lane 3: Immunoblot of SP-1 cells using monoclonal mouse anti-IP_3R3 antibody.

(As a control, SP-1 cells were immunobloted with normal mouse IgG. No signal was detected in these samples-data not shown).

Fig.7: Measurement of IP_3 Receptor Phosphorylation by ROK.

The kinase reaction was carried out in the reaction mixture containing 100μM [γ-^{32}P]ATP (15-600 mCi/mmol), purified ROK (isolated from anti-ROK-conjugated beads)] and 1 μg cellular proteins (e.g. IP_3R1, IP_3R2, IP_3R3 and myelin basic protein) in the presence of GTPγS•GST-RhoA (1 μM) or GST-RhoA (1 μM) as described in the Materials and Methods.

A: Phosphorylation of IP_3 receptor Subtypes by ROK *in vitro*.

Lane 1: Autoradiogram of IP_3R1 phosphorylation by ROK (isolated from SP-1 cells) treated with GST-RhoA.

Lane 2: Autoradiogram of IP_3R2 phosphorylation by ROK (isolated from SP-1 cells) treated with GST-RhoA.

Lane 3: Autoradiogram of IP_3R3 phosphorylation by ROK (isolated from SP-1 cells) treated with GST-RhoA.

Lane 4: Autoradiogram of IP_3R1 phosphorylation by ROK (isolated from SP-1 cells) activated by GTPγS•GST-RhoA.

Lane 5: Autoradiogram of IP_3R2 phosphorylation by ROK (isolated from SP-1 cells) activated by GTPγS•GST-RhoA

Lane 6: Autoradiogram of IP_3R3 phosphorylation by ROK (isolated from SP-1 cells) activated by GTPγS•GST-RhoA.

B: Stoichiometry analysis of IP3 receptor subtype phosphorylation by Rho-Kinase (ROK).

The kinase reaction used in these experiments was the same as described in the legend of Fig. 7A. The amount of [γ-^{32}P]ATP incorporated into IP_3 recerptor subtypes and myelin basic

protein by ROK (in the presence of activated GTPγS•GST-RhoA or unactivated GST-RhoA) was measured at 2h as described in the Materials and Methods.
a: The amount of ^{32}P incorporated into IP_3R1 by ROK activated by GTPγS•GST-RhoA.
b: The amount of ^{32}P incorporated into IP_3R2 by ROK activated by GTPγS•GST-RhoA.
c: The amount of ^{32}P incorporated into IP_3R3 by ROK activated by GTPγS•GST-RhoA.
d: The amount of ^{32}P incorporated into myelin basic protein by ROK activated by GTPγS•GST-RhoA.

Fig. 8: Measurement of [^{3}H]-IP3 Binding of Unphosphorylated and ROK Phosphosphorylated IP_3 Receptor Subtypes.

To determine [^{3}H]-IP_3 binding, IP_3 receptor subtype (unphosphorylated or ROK phosphorylated IP_3R1, IP_3R2 or IP_3R3-associated beads) were incubated with a solution containing 25 mM sodium phosphate (pH 7.4), 100 mM KCl, 20 mM NaCl, 1 mM EDTA, 1 mg/ml BSA, 0.05% Triton X-100 and 0.01 mCi [^{3}H]-IP_3 (38 Ci/mmol, Amersham Co.) in the presence of various concentration of unlabeled IP_3 in a final volume of 50 ml at 4°C for 2 h with constant agitation as described in the Materials and Methods. The binding reaction was terminated by adding 200 µl of cold phosphate-buffered saline (pH 7.4) and filtrating through GF/B glass fiber filters (Millipore Co., Bedfored, MA). The filter-associated radioactivity was analyzed by liquid scintillation counting as described in the Materials and Methods. The numbers shown in the results were the averages of triplicate determinants in 3 experiments, which varied by less than 5%.
B: Measurement of $^{45}Ca^{2+}$ Flux in Phospholipid Vesicles (Liposomes) Containing IP_3 Receptor Subtypes.

Purified IP_3 receptor subtypes (obtained from anti-IP_3R1, IP_3R2 or IP_3R3 immuno-beads) (25µg/ml) were incorporated into phosphatidylcholine/phosphatidylserine vesicles liposomes). These IP_3 receptor subtype-containing phospholipid vesicles (liposomes) were then processed for phosphorylation (in the presence of ROK activated by GTPγS•GST-RhoA or ROK treated with GST-RhoA alone) and used for the measurement of IP_3-induced $^{45}Ca^{2+}$ influx as described in the Materials and Methods. a: The amount of IP_3-induced $^{45}Ca^{2+}$ flux in unphosphorylated (□) or ROK-phosphorylated (■) IP_3R1-containing vesicles. b: The amount of IP_3-induced $^{45}Ca^{2+}$ flux in unphosphorylated (□) or ROK-phosphorylated (■) IP_3R2-containing vesicles. c: The amount of IP_3-induced $^{45}Ca^{2+}$ flux in unphosphorylated (□) or ROK-phosphorylated (■) IP_3R3-containing vesicles.

Fig. 9: Analyses of HA-Induced *In Vivo* Phosphorylation of IP_3 Receptor Subtypes (A) and Ca^{2+} Mobilization (B) In SP-1 Transfectants.
A: *In Vivo* Phosphorylation of IP_3 Receptor Subtypes: Both vector-transfected or ROK-PHcDNA-transfected SP-1 cells were metabolically labeled with $H_3{}^{32}PO_4$. Subsequently, these radioactively labeled transfectants (treated with 50µg/ml HA or without any HA treatment) were solubilized by 1% NP-40 and immunoprecipitated with mouse anti-IP_3R1, anti-IP_3R2 or IP_3R3 antibody followed by goat-anti-mouse IgG-conjugated beads, respectively. These immunoprecipitated materials were then boiled in SDS-sample buffer and subjected to SDS-PAGE. The protein bands were revealed by silver stain and the radiolabeled bands were visualized by fluorography as described in the Materials and Methods.

a: Autoradiogram of IP_3R1 (lane 1), IP_3R2 (lane 2), or IP_3R3 (lane 3) phosphorylation in vector-transfected cell treated with no HA; Autoradiogram of IP_3R1 (lane 4), IP_3R2 (lane 5), or IP_3R3 (lane 6) phosphorylation in vector-transfected cells treated with HA.
b: Autoradiogram of IP_3R1 (lane 1), IP_3R2 (lane 2) or IP_3R3 (lane 3) phosphorylation in ROK-PHcDNA tranfected cells treated with no HA; Autoradiogram of IP_3R1 (lane 4), IP_3R2 (lane 5) or IP_3R3 (lane 6) phosphorylation in ROK-PHcDNA transfected cells treated with HA.
B: HA-Mediated Ca^{2+} Mobilization.

Intracellular Ca^{2+} mobilization was measured by a fluorescence spectrophotometer using cells [transfected with ROK-PHcDNA (b) or vector alone (a)] loaded with Fura-2/AM as described in the Materials and Methods. Subsequently, Fura-2 labeled transfectants were then treated with HA (indicated by arrow head). The insert of (b) illustrates Ca^{2+} release from internal stores by ionomycin and an inhibition of Ca^{2+} elevation by EGTA (indicated by arrows) in ROK-PHcDNA-transfected cells preincubated with 1.2mM $CaCl_2$.

Fig. 10: A proposed model for the interaction between CD44v10 and Rho-Kinase (ROK) and its role in promoting IP_3 receptor-mediated Ca^{2+} signaling and HA-mediated breast tumor cell migration.

The binding of HA to CD44v10 isoform (containing the v10 exon-encoded structure) induces CD44v10 interaction with Rho-Kinase (ROK) which, in turn, phosphorylates IP_3 receptors and induces internal Ca^{2+} release leading to cytoskeleton activation and HA-mediated breast tumor cell migration.

Figure 1

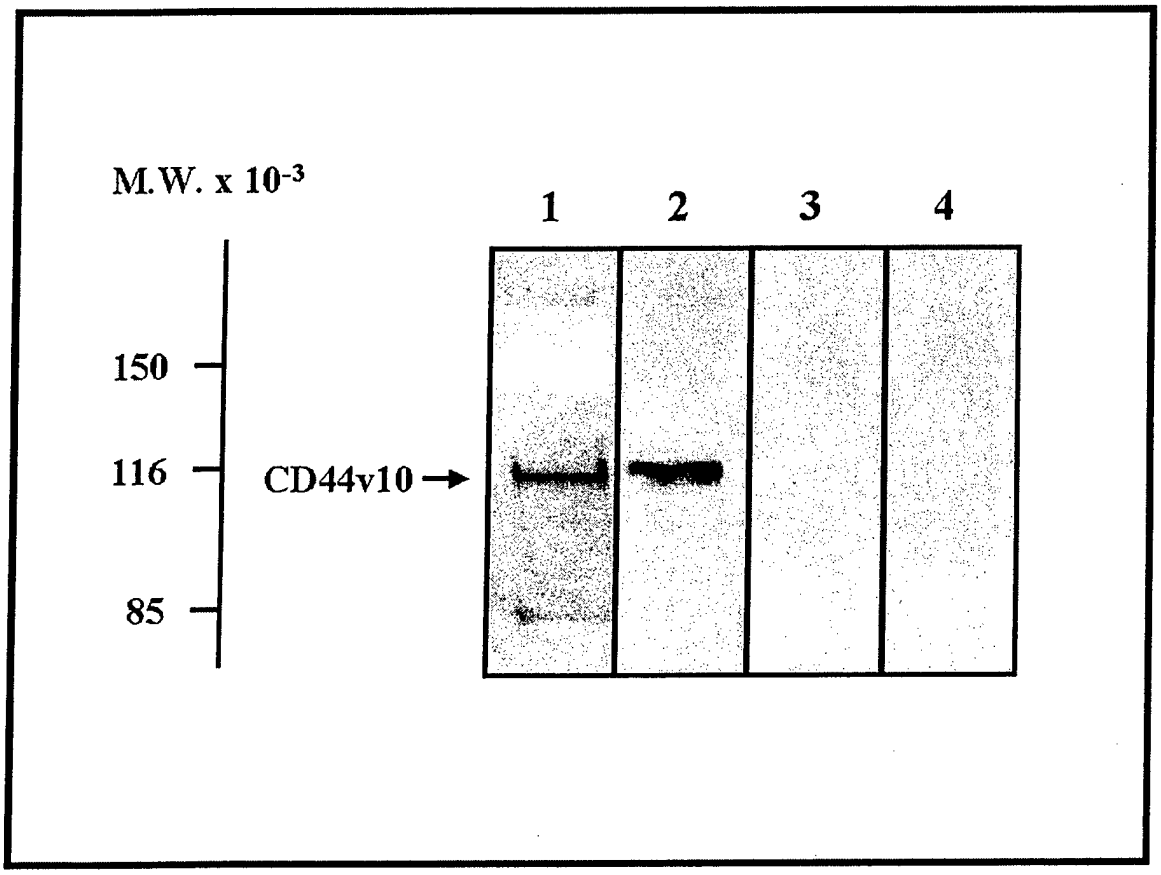

Figure 2

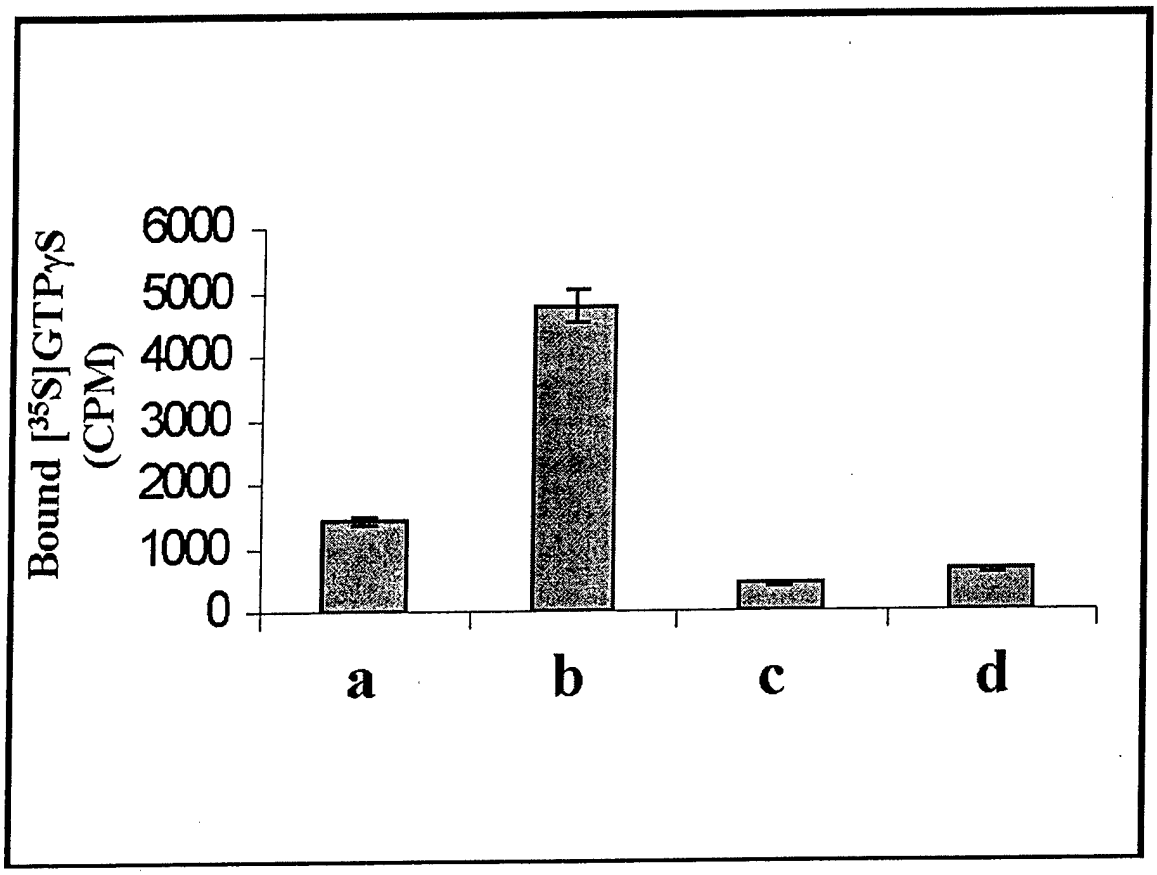

Figure 3

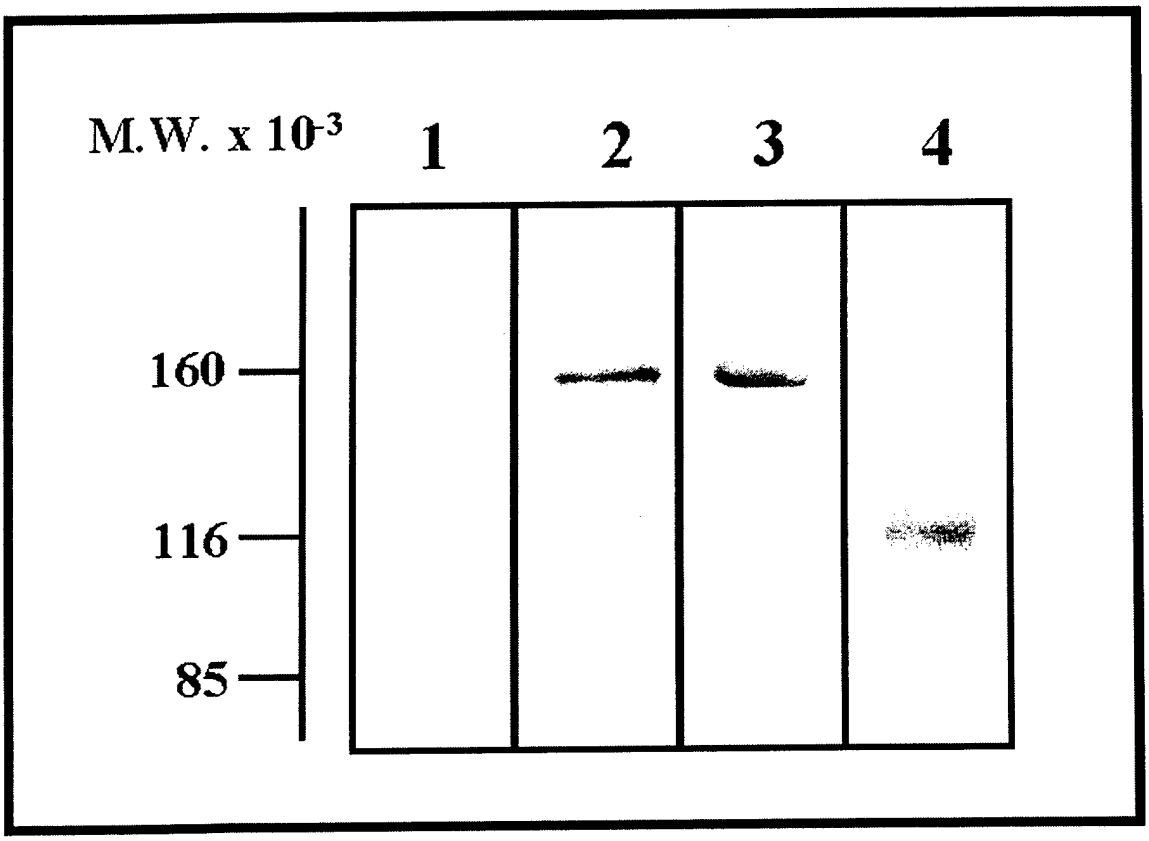

Figure 4

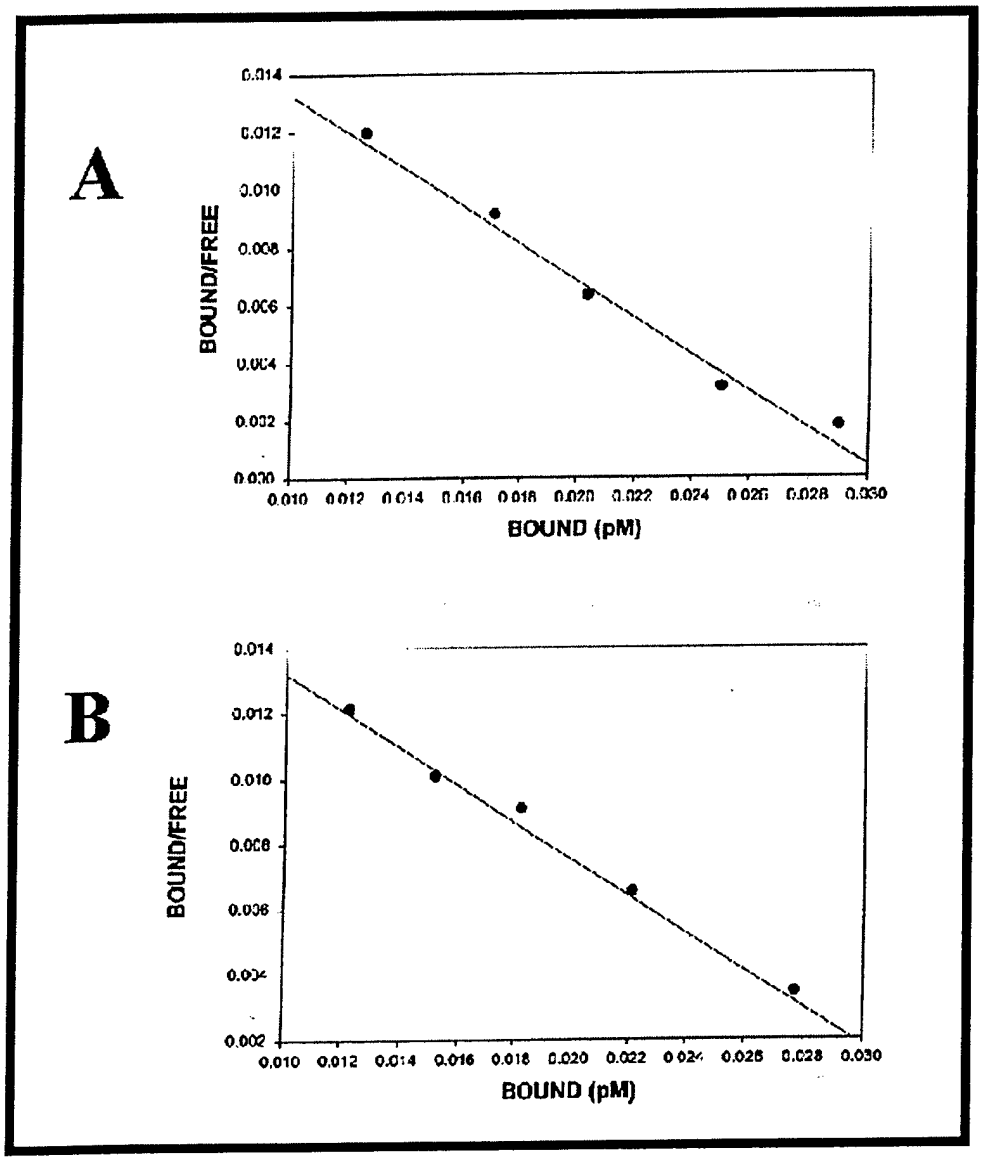
A
BOUND/FREE
0.014
0.012
0.010
0.008
0.006
0.004
0.002
0.000
0.010 0.012 0.014 0.016 0.018 0.020 0.022 0.024 0.026 0.028 0.030
BOUND (pM)
B
BOUND/FREE
0.014
0.012
0.010
0.008
0.006
0.004
0.002
0.010 0.012 0.014 0.016 0.018 0.020 0.022 0.024 0.026 0.028 0.030
BOUND (pM)

Figure 5

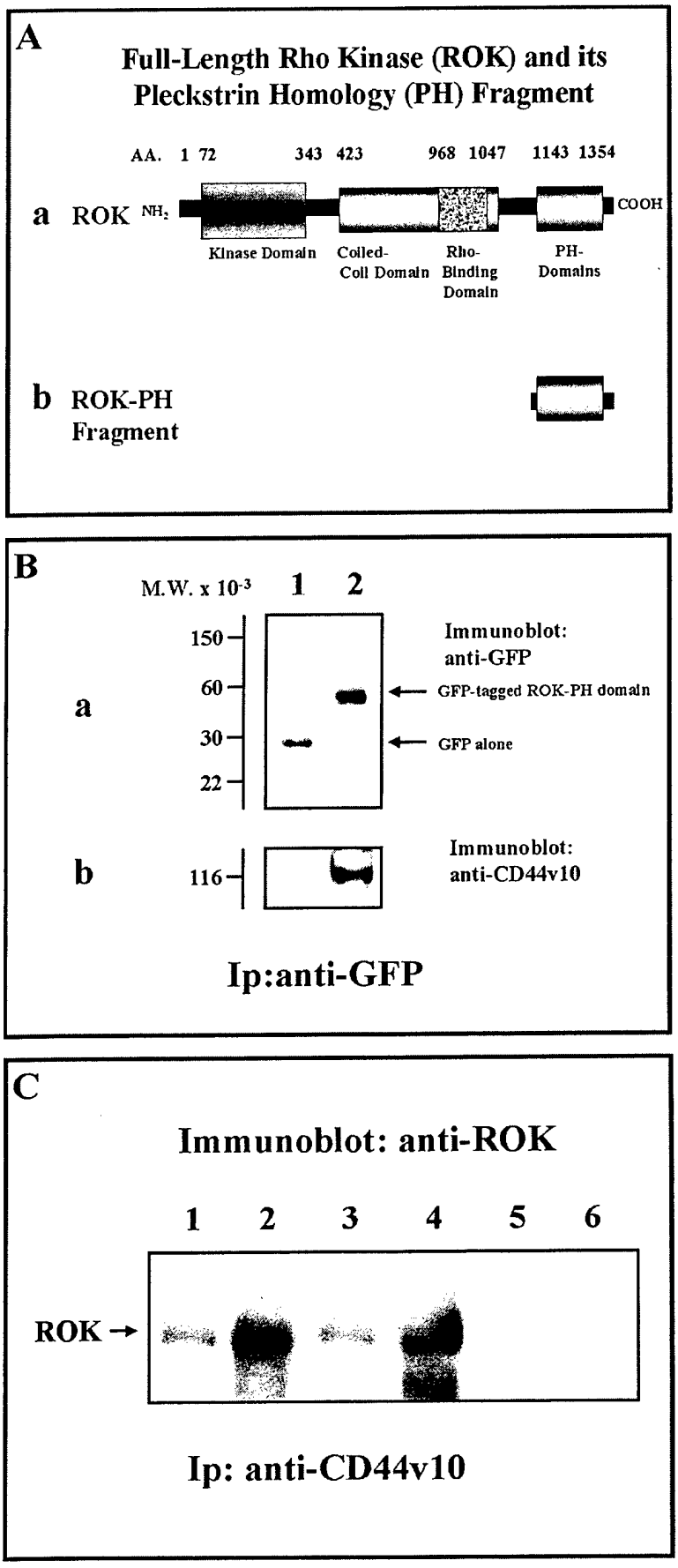
A
Full-Length Rho Kinase (ROK) and its Pleckstrin Homology (PH) Fragment
AA. 1 72 343 423 968 1047 1143 1354
a ROK NH2
COOH
Kinase Domain
Coiled-Coil Domain
Rho-Binding Domain
PH-Domains
b ROK-PH Fragment
B
M.W. x 10-3
1 2
150
60
30
22
a
Immunoblot: anti-GFP
GFP-tagged ROK-PH domain
GFP alone
b
116
Immunoblot: anti-CD44v10
Ip:anti-GFP
C
Immunoblot: anti-ROK
1 2 3 4 5 6
ROK
Ip: anti-CD44v10

Figure 6

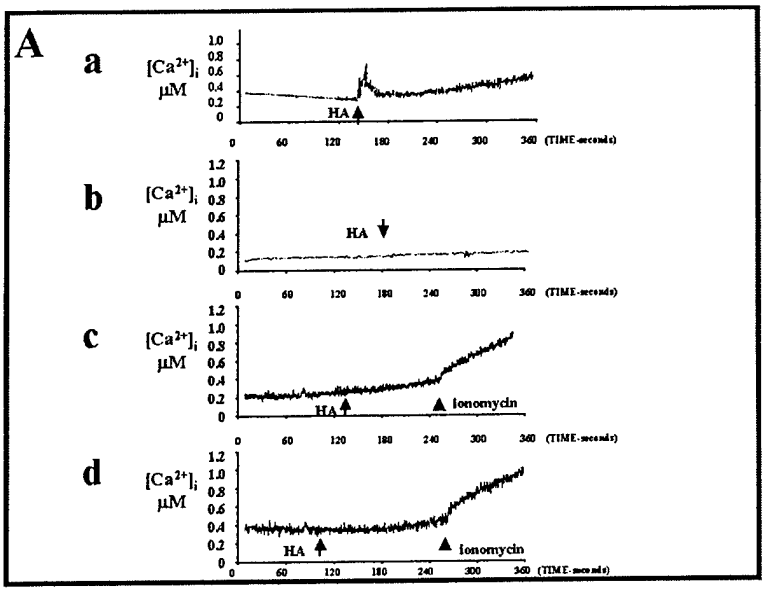
A
a
b
c
d
[Ca2+]i µM
HA
Ionomycin
(TIME-seconds)

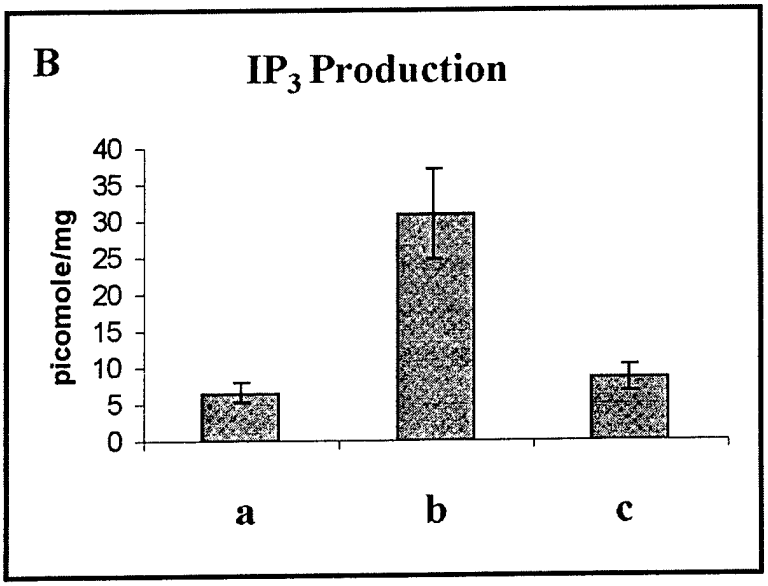
B
IP3 Production
picomole/mg
40
35
30
25
20
15
10
5
0
a
b
c

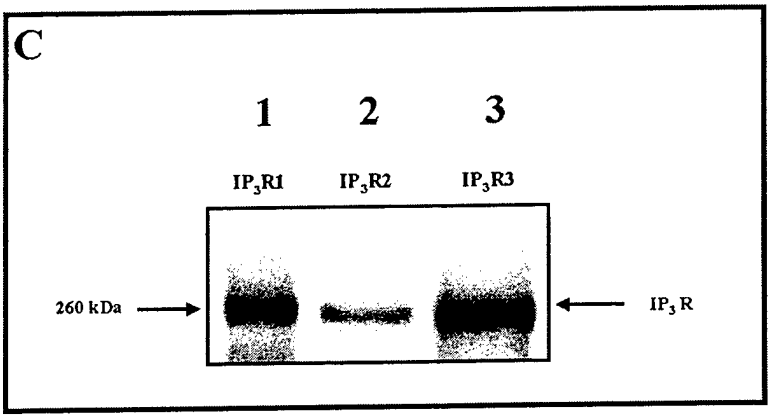
C
1
2
3
IP3R1
IP3R2
IP3R3
260 kDa
IP3 R

Figure 7

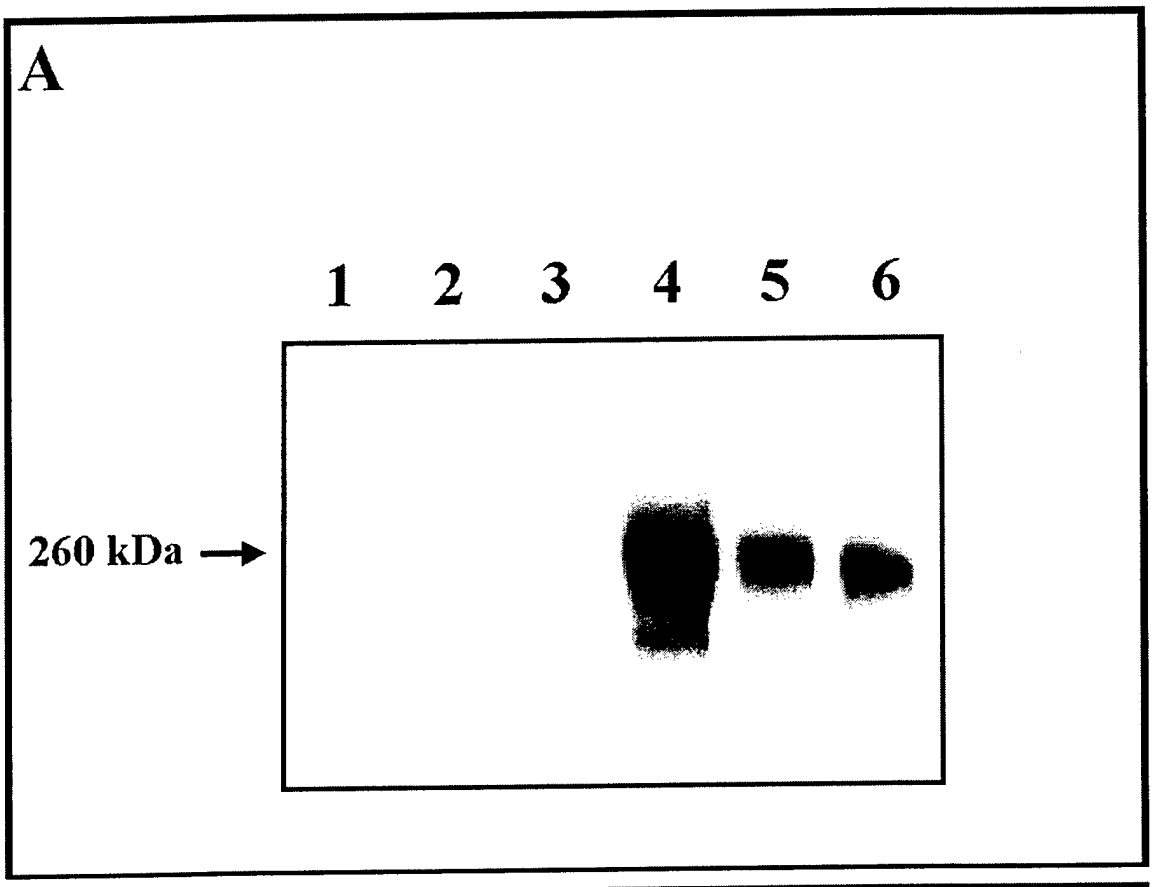
A
1 2 3 4 5 6
260 kDa
B
mol 32P incorporated/ mol IP3Rs
1.0
0.8
0.6
0.4
0.2
0
IP3R1
IP3R2
IP3R3
MBP
a
b
c
d

Figure 8

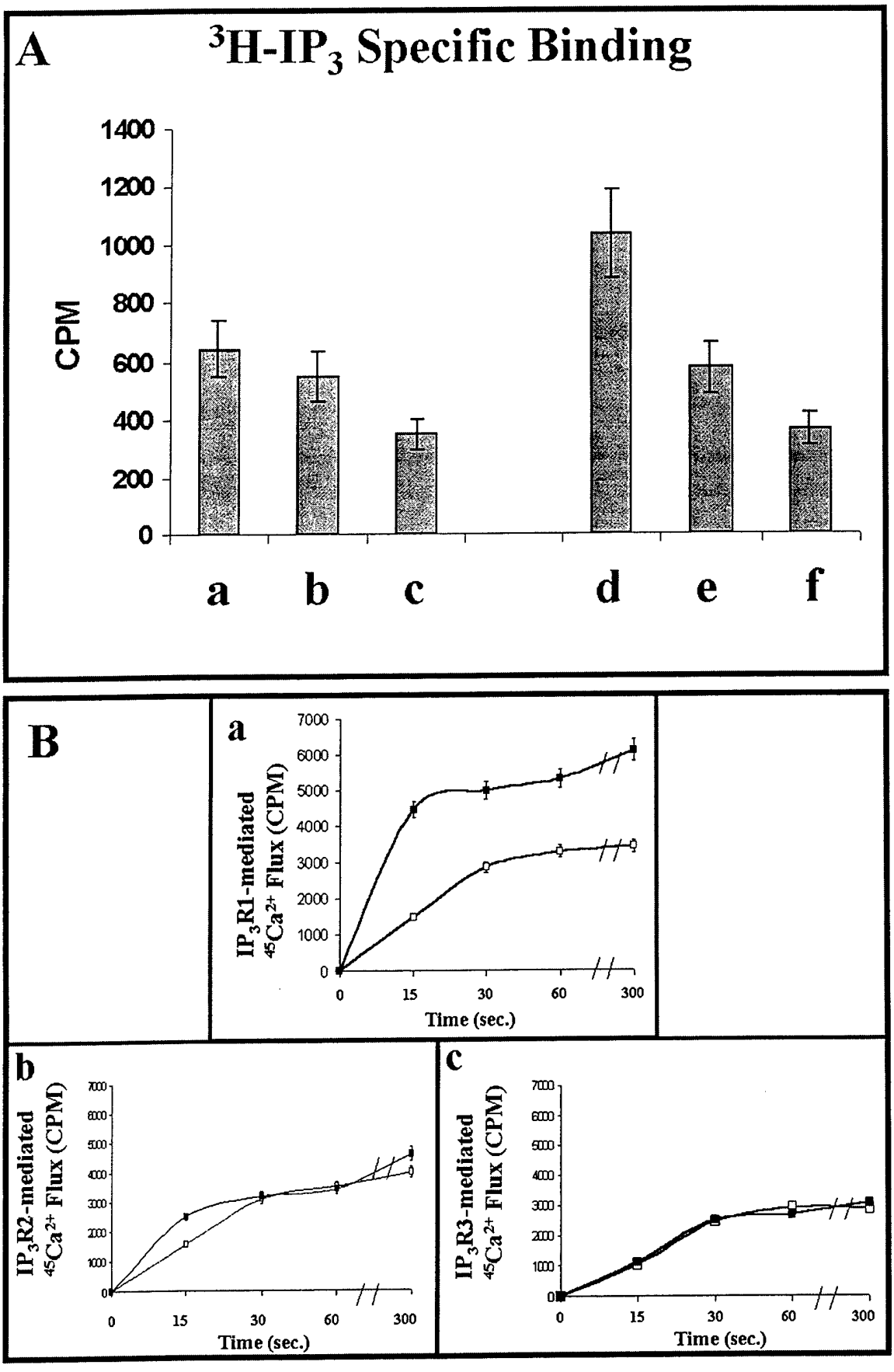
A
^{3}H-IP$_3$ Specific Binding
CPM
1400
1200
1000
800
600
400
200
0
a
b
c
d
e
f
B
a
IP$_3$R1-mediated $^{45}Ca^{2+}$ Flux (CPM)
7000
6000
5000
4000
3000
2000
1000
0
0
15
30
60
300
Time (sec.)
b
IP$_3$R2-mediated $^{45}Ca^{2+}$ Flux (CPM)
Time (sec.)
c
IP$_3$R3-mediated $^{45}Ca^{2+}$ Flux (CPM)
Time (sec.)

Figure 9

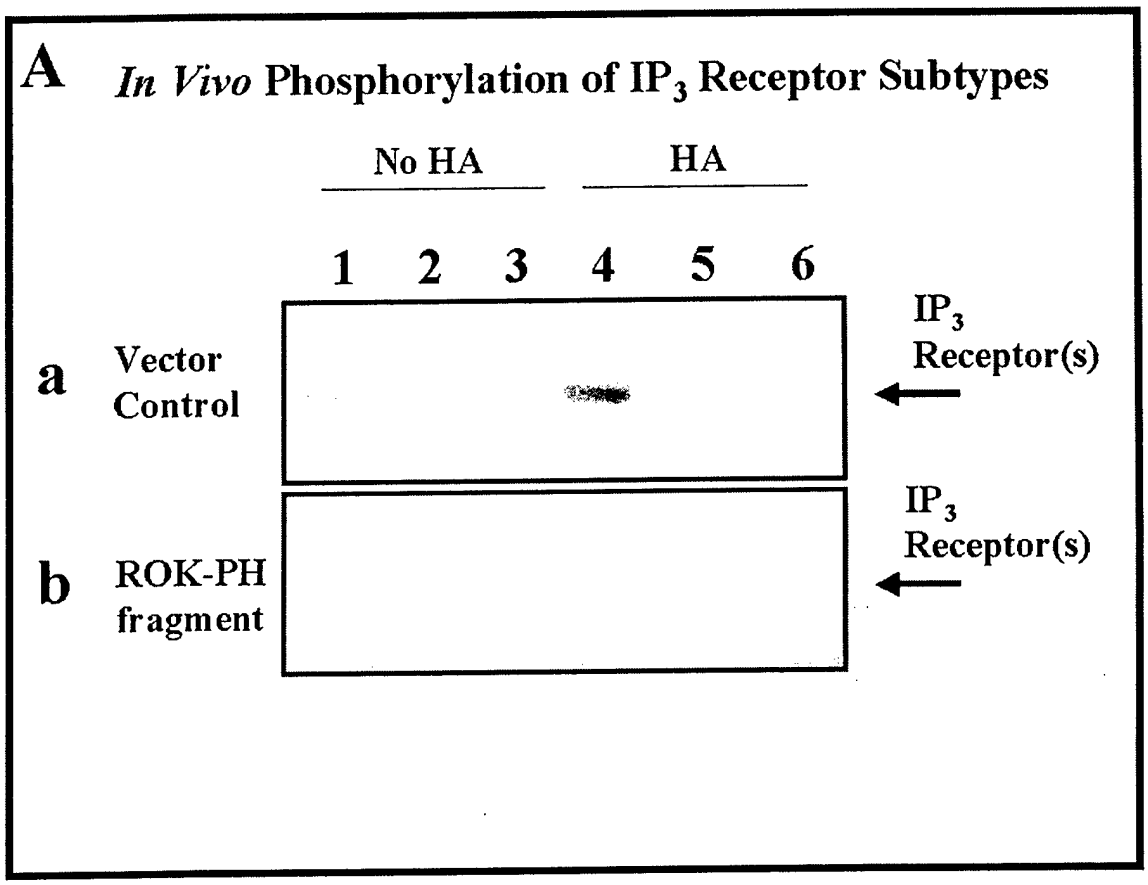
A
In Vivo Phosphorylation of IP3 Receptor Subtypes
No HA
HA
1 2 3 4 5 6
a
Vector Control
IP3 Receptor(s)
b
ROK-PH fragment
IP3 Receptor(s)

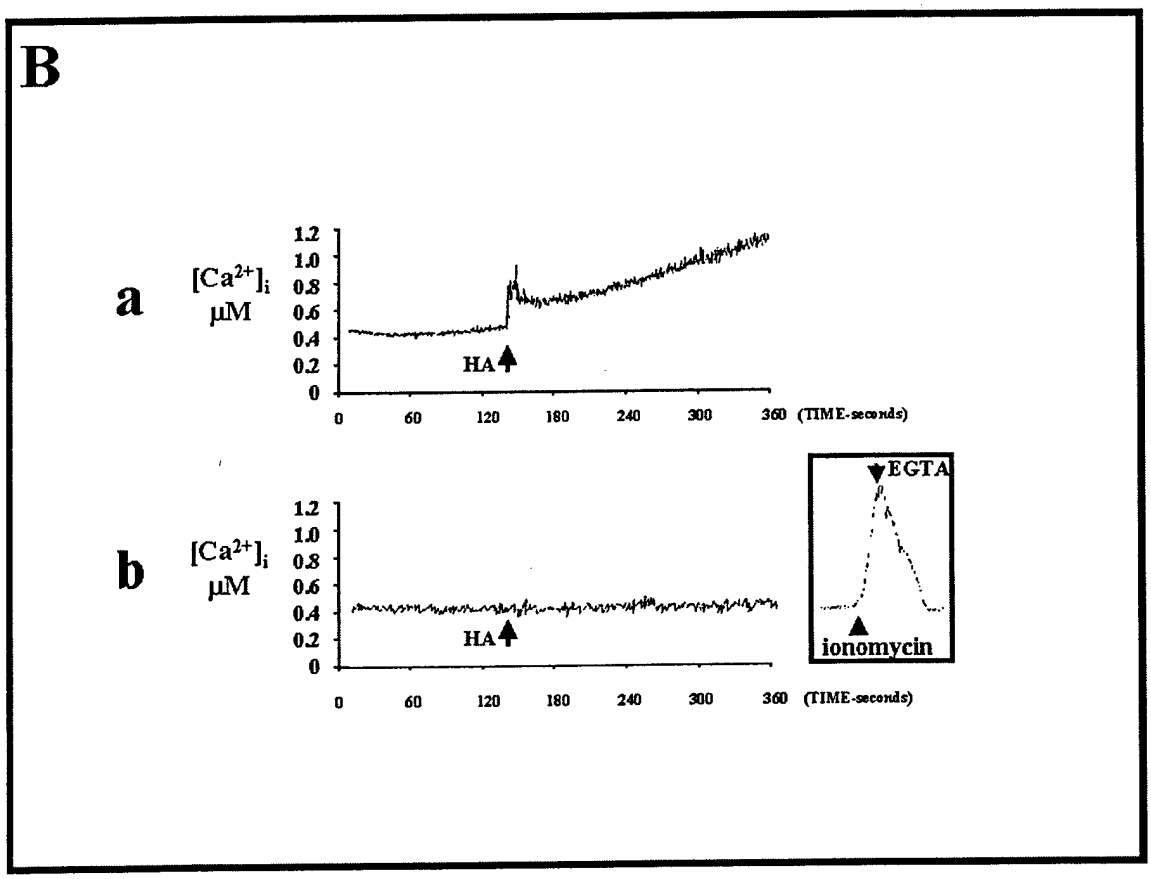
B
a
[Ca2+]i µM
1.2
1.0
0.8
0.6
0.4
0.2
0
HA
0 60 120 180 240 300 360 (TIME-seconds)
b
[Ca2+]i µM
EGTA
ionomycin
HA
0 60 120 180 240 300 360 (TIME-seconds)

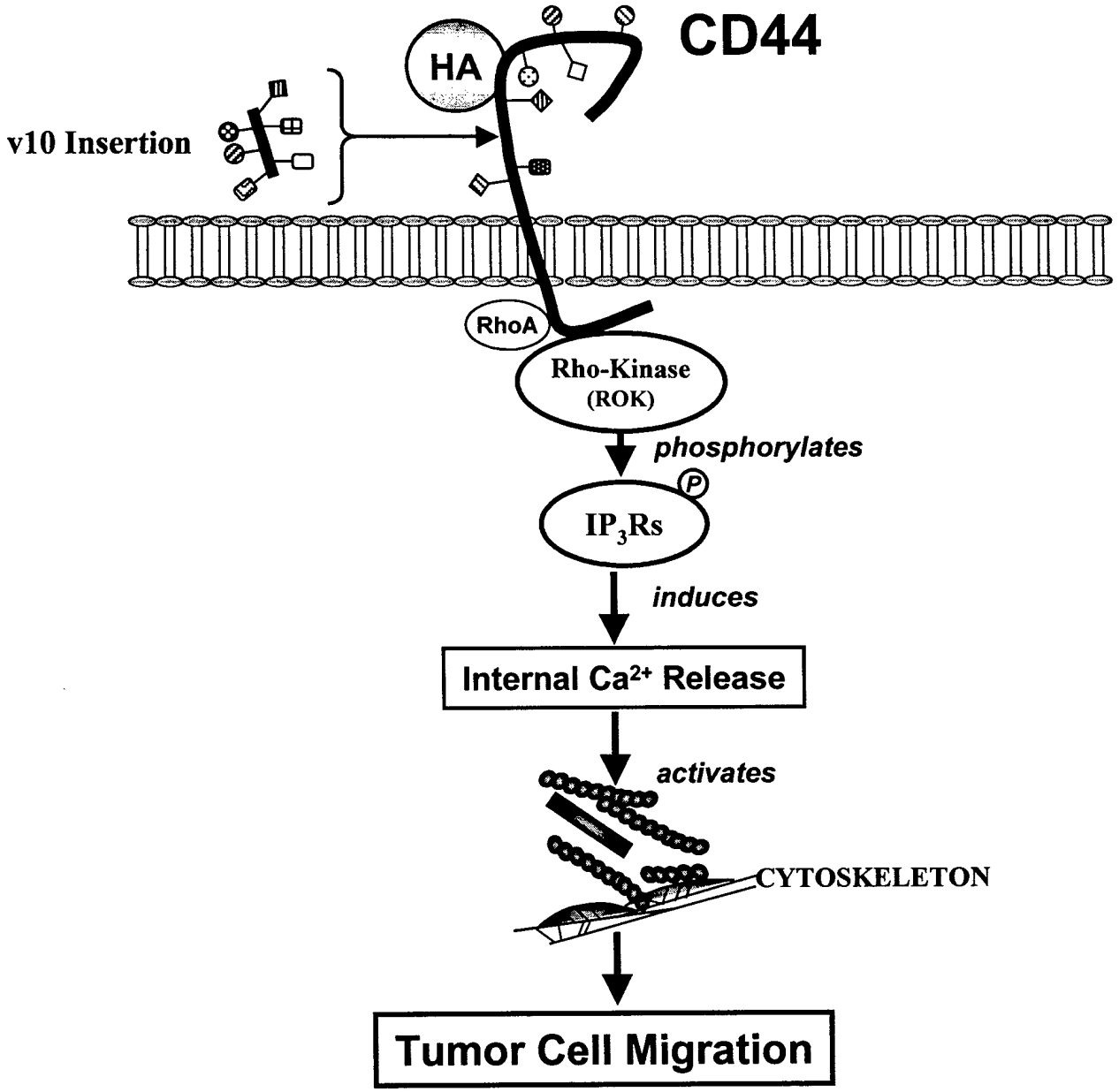

Bourguignon, Lilly, PhD

Table 1: Measurement of HA-Dependent and CD44v10-Specific Breast Tumor Cell Migration.
A: Effects of Anti-CD44 Antibody on HA-Dependent and CD44v10-Specific Breast Tumor Cell Migration.

Treatments	**Migratory Cells *(% of total cells)***
No treatment (control)	10
HA treatment	50
Anti-CD44 IgG pretreatment + HA treatment	5

B: Effects of Various Drugs on HA-Dependent and CD44v10-Specific Breast Tumor Cell Migration.

Treatments	**Migratory Cells *(% of total cells)*[a]**
No drug treatment (control) + HA	49
Colchicine treatment + HA	48
Cytochalasin D treatment + HA	11
W-7 treatment + HA	13
Xetospongin C treatment + HA	10
BAPTA treatment + HA	12

C: Effect of Overexpression of ROK-PH Domain on HA-Dependent and CD44v10-Specific Breast Tumor Cell Migration.

Cells	Migratory Cells *(% of total cells)*[a]	
	No HA Addition	HA Addition
Untransfected cells (control)	10	50
Vector-transfected cells	11	49
ROK-PHcDNA-transfected cells	10	12

a: Breast tumor cells (SP-1 cells) [~1 x 10^4 cells/well in phosphate buffered saline (PBS), pH 7.2] were placed in the upper chamber of the transwell unit. In some cases, SP-1 cells were pretreated with various agents (e.g. anti-CD44 IgG, cytochalasin D, colchicine, W-7, Xetospongin C or BAPTA) or transfected with either ROK-PHcDNA, or vector alone. After 18h incubation at 37°C in a humidified 95% air/5% CO_2 atmosphere, cells on the upper side of the filter were removed by wiping with a cotton swap. Cell migration was determined by measuring the % of total cells that migrated to the lower side of the polycarbonate filters containing hyaluronan (HA) (or no HA) by standard cell number counting assays as described in the Materials and Methods. The CD44-specific cell migration was determined by subtracting non-specific cell migration (i.e. cells migrate to the lower chamber in the presence of rat anti-CD44 antibody treatment) from the total migratory cells in the lower chamber. Each assay was set up in triplicate and repeated at least 3 times. All data were analyzed statistically using the Student's t test and statistical significance was set at $p<0.01$.

BINDING: We have prepared the report according to the instruction provided by DOD.